

RESEARCH MEMORANDUM

AN INVESTIGATION OF EFFECTS OF FLAME-HOLDER GUTTER

SHAPE ON AFTERBURNER PERFORMANCE

By S. Nakanishi, W. W. Velie, and L. Bryant

Lewis Flight Propulsion Laboratory
Cleveland, Ohio

NATIONAL ADVISORY COMMITTEE
FOR AERONAUTICS

WASHINGTON
February 10, 1954

Declassified August 19, 1960

NATIONAL ADVISORY COMMITTEE FOR AERONAUTICS

RESEARCH MEMORANDUM

AN INVESTIGATION OF EFFECTS OF FLAME-HOLDER GUTTER

SHAPE ON AFTERBURNER PERFORMANCE

By S. Nakanishi, W. W. Velie, and L. Bryant

SUMMARY

The effect of flame-holder gutter cross-sectional shape on afterburner performance was investigated in an afterburner test rig which was 26 inches in diameter. The fuel-air distribution and burner inlet temperature (approximately 1250° F) were held as nearly constant as possible, and the arrangement of flame-holder gutter elements was the same for all gutter shapes. Each flame holder was investigated over a wide range of fuel-air ratio, burner inlet velocity, and burner inlet pressure. Variations in burner inlet velocity were obtained by using choked exhaust nozzles with different throat sizes. Variations in burner inlet pressure were obtained by varying the afterburner air flow. Burner inlet velocities ranging from 380 to 700 feet per second and burner inlet pressures ranging from 6 to 20 inches of mercury absolute were covered during the investigation.

In general, the combustion efficiency ranged from 90 percent at a burner inlet velocity of 400 feet per second and a burner inlet pressure of 15 inches of mercury to 60 percent at a burner inlet velocity of 700 feet per second and a burner inlet pressure of 8 inches of mercury. A channel-shaped gutter with a rounded upstream face had a combustion efficiency which was 7 percentage points poorer than that for the conventional V-gutter. A flame holder with vortex generators at the trailing edges had a combustion efficiency which was 3.5 percentage points better than that for the conventional V-gutter. Flame-holder shape did not greatly affect combustion limits. Turbulence produced by the addition of upstream vortex generators to a conventional V-gutter flame holder appeared to have a slight adverse effect on the lean limit of combustion. A channel-shaped gutter with a flat upstream face and a conventional V-gutter which had sharp-edged tabs at the trailing edge gave the highest pressure losses both with and without afterburning.

INTRODUCTION

In many cases of current turbojet power plants for aircraft, the need for thrust augmentation during certain periods of flight operation dictates the use of afterburners. More extensive needs have arisen in aircraft designed for transonic and supersonic flight. Some of the performance characteristics desirable in afterburners for such aircraft are high combustion efficiency at low pressures, stable combustion over a wide range of fuel-air ratio, and low internal drag to keep tail-pipe pressure loss and, hence, thrust loss to a minimum, particularly during nonburning operation, such as in cruise flight.

As has been shown in numerous afterburner investigations, references 1 to 3, for example, increasing burner inlet velocity and decreasing burner pressure have deleterious effects on both combustion efficiency and stability limits. Efforts to minimize the harmful effects on afterburner performance at increasing velocity and decreasing pressure or to improve performance at given conditions of operation have been centered primarily about design of the fuel injection system, the inlet diffuser, and the flame-holder blockage or gutter width. The afterburners of references 1 to 3 and other afterburners have generally used flame holders made up of gutter elements having a V, an H, or a semicircular cross section. Investigations of the effects of systematic changes in gutter shape on afterburner performance have been limited in scope, however.

Published literature on basic studies of flame stabilization and propagation such as references 4 and 5 reported stability limits to be a function of approach stream velocity and gutter width. In reference 5 it was postulated that hot burned gases in the recirculation zones immediately behind the flame holders raised the temperature of the approaching mixture and provided continuous ignition. Although the studies of both references 4 and 5 indicate that blow-out velocity was independent of the particular stabilizer shapes tested over the range of conditions covered by the investigations, it appeared that radical changes in gutter shape which would strongly affect the character of recirculation behind the gutter might correspondingly affect the limits of flame stabilization. It was possible also that the degeneration of combustion performance at the low pressure and high velocity flow conditions encountered in afterburner operation might be partially dependent upon the shape of the flame-holder gutter elements.

An investigation of the isothermal wake flow characteristics behind various gutter shapes was accordingly conducted and is reported in reference 6. The gutter shape altered the frequency and strength of vortices shed from the body in the absence of combustion. An attempt was made to relate the flow characteristics with parameters which might be indicative of the amount of recirculatory mass flow behind the gutter, and which might in turn have some bearing upon the combustion process

utilizing bluff-body flame stabilizers. The exact mechanism of flame stabilization and its relation to nonburning aerodynamic properties of various gutter shapes were not known, however.

An experimental investigation that included gutter shapes similar to those of reference 6 was therefore conducted at the NACA Lewis laboratory in a large-scale simulated afterburner test rig to study the effect of flame-holder gutter shape on combustion performance and its possible relation to the wake flow characteristics found during the nonburning tests. All gutter shapes were 1.5 inches wide. The same geometrical arrangement of gutter elements was used for all flame holders. The inlet gas temperature was held constant, and the fuel-air distribution was held as near as possible to a uniform mixture.

A total of 10 gutter shapes was investigated. Burner inlet velocities ranged from 380 to 700 feet per second, and burner inlet pressures ranged from 6 to 20 inches mercury absolute. Afterburner fuel-air ratio ranged from lean blow-out to either rich blow-out or a fuel-air ratio of approximately 0.08. Data are presented to show the effect of these variables on combustion performance.

APPARATUS

Installation

The general arrangement of the full-scale afterburner installation and a detailed sketch of the burner are shown in figure 1. Combustion air (fig. 1(a)) was supplied to the preheater at approximately 80° F, and was heated to a temperature of 1250° F before entering the gas mixing chamber. The preheater, which simulated a primary turbojet engine combustor, consisted of eight J35 combustor cans. Upon leaving the preheater the hot gas was thoroughly diffused in the mixing chamber to promote a uniform temperature distribution before entering the diffuser. A 44-percent-solidity screen was placed at the diffuser entrance to insure a uniform velocity profile at this station.

The diffuser inner body was designed for a constant rate of area increase except at the discharge end where the rate of area change increased because of rounding-off the end of the inner body. The inner body was supported by four streamlined struts which separated the diffuser into four channels extending from the diffuser inlet to station 2. The installation of the various flame holders was accomplished by the removal of an accessible spool piece to which the flame holders were attached. A quartz window 3 inches wide and 6 inches long was placed in the spool section to provide a means of observing the flame front during combustion and to facilitate recording blow-outs. An internal view of the burner showing details of the diffuser contours, the

spray bar, and the flame-holder locations is shown in figure 1(b). The burner was 25.75 inches in diameter (inside dimension) and approximately 53 inches long. The fuel injectors, which were installed in the diffuser section, consisted of 24 radial spray bars equally spaced around the circumference of the diffuser and located 29.5 inches upstream of the flame holder. Each spray bar contained eight orifices 0.020 inch in diameter, as shown in figure 2. In some phases of the investigation where higher air flows were encountered, spray bars with orifices 0.030 inch in diameter were employed in an endeavor to maintain comparable magnitudes of fuel manifold pressure. The fuel was injected normal to the air stream at all times.

Flame holders. - Ten different flame holders, the details of which are shown in figure 3, were used in the investigation. Figure 3(a) shows the arrangement of gutters which was characteristic of all the flame holders used. The flame holders, which were supported by four radial streamlined struts, were composed of 2 annular gutters with mean diameters of 9.5 and 18.5 inches, interconnected by four radial gutters of the same shape as that of the annular gutters. The width of the gutter elements was 1.5 inches and the projected blockage, exclusive of streamlined supporting struts, was 29 percent of the burner cross-sectional area.

Details of the gutter cross-sectional shapes used with the various flame holders are shown in figure 3(b). Flame holder 1 had the conventional V-gutter. Flame holder 2 had a channel gutter with a flat upstream face. Numbers 3 and 4 had sharp-edged and round-edged tabs, respectively, mounted along the trailing edges of V-shaped gutters. Number 5 had a cambered V-gutter and 6, a conventional V-gutter with vortex generators mounted upstream of the leading edge. Number 7 had a V-gutter with a crescent-shaped element 0.5 inch wide attached to the trailing edges of the gutter. Flame holder 8 had a conventional V-gutter with vortex generators mounted on the sides of the gutter. Number 9 had the combined features of flame holders 5 and 6 with vortex generators mounted upstream of a cambered V-gutter. Number 10 had features similar to 2, except that the upstream face was semicircular and the over-all length of the gutter was increased 0.75 inch. The included angles of the V-type gutters were decreased from 34° to 30° in some cases to accommodate the tabs at the gutter lip. The spacing at the vortex generators for flame holders 6, 8, and 9 is shown in figure 3(c).

Exhaust nozzles. - Converging-diverging exhaust nozzles with three different throat sizes were used to cover a range of burner inlet velocities. The divergent section of the exhaust nozzles downstream of the throat was used to induce choking at the throat under some conditions of marginal exhaust system capacity. The nozzles differed only in throat

area and angles of divergence. The percentages of throat area to burner cross-sectional area for the three nozzles were 52.2, 70, and 82 percent, which, for choked flow, gave ranges of burner inlet velocities from approximately 380 to 450 feet per second, 500 to 600 feet per second, and 580 to 700 feet per second, respectively. The higher velocities for each nozzle were obtained at fuel-air ratios in the region of lean blow-out and the lower velocities, in the vicinity of rich blow-out. The nozzles were capable of remaining choked down to an over-all nozzle pressure ratio (ratio of nozzle inlet pressure to nozzle exhaust pressure) of 1.25.

Instrumentation

Pressure and temperature measurements were taken at various stations throughout the setup, as shown in figure 1(b). More specific details of the instrumentation at some of the stations are shown in figure 4. Twenty-five Franz-type chromel-alumel thermocouples were located at station 2 for recording afterburner inlet total temperature. The arrangement of the thermocouples at this station is shown in figure 4(a).

At the burner inlet, station 4, 26 total-pressure probes, 4 stream static probes, and 8 wall static taps were located as shown in figure 4(b). Accommodations were also made at station 4 for inserting a fuel-air ratio sampling probe in 4 circumferential positions. The fuel-air ratio sampling probe was made of 3/16 inch Inconel tubing with a 0.032 inch wall thickness; the probe inlet faced directly into the fuel-air stream. The probe moved on a radial line from the wall of the burner to a point 11.25 inches from the wall. The fuel-air ratio of the sample drawn from the burner was determined by an NACA analyzer described in reference 7.

A water-cooled total-pressure rake was located at the burner outlet, station 5. Twelve copper probes spaced on equal areas and arranged as shown in figure 4(c) were used. In addition to the total-pressure rake at station 5, two wall static taps were located at this station diametrically opposite each other.

PROCEDURE

The preheater supplied air heated to 1250° F to the afterburner inlet. With the air flow set and the afterburner inlet temperature at 1250° F, the exhaust nozzle was unchoked to raise the burner inlet pressure and to lower the inlet velocity. The afterburner was then ignited at a burner fuel-air ratio of approximately 0.050 by use of a torch-type ignitor ahead of the flame holder. After ignition was complete, the torch ignitor was shut off and the exhaust nozzle was choked by decreasing exhaust pressure. With the exhaust nozzle choked, runs with constant

air flow were made at different fuel flows to vary fuel-air ratio. Air flow was set and maintained constant for a given series of runs by a choked valve in the air supply line upstream of the test facility. The fuel-air ratio range covered was from lean blow-out to rich blow-out or to a fuel-air ratio of 0.080, whichever occurred first. Large step changes in inlet pressure were obtained by making runs at different air flows, and large step changes in inlet velocity were made by using exhaust nozzles of different throat area. At a given air flow, changes in fuel-air ratio resulted in small changes in both inlet velocity and inlet pressure due to the changes in temperature rise. The range of conditions covered for each flame holder is summarized in table I. All flame-holder shapes were investigated at an inlet velocity level of 500 to 600 feet per second and some of the flame-holder shapes were investigated at two other velocity levels. During the investigation a range of velocities from 380 to 700 feet per second and a range of pressures from 6 to 20 inches of mercury absolute were covered.

Isothermal pressure drops (afterburner inoperative) at different inlet velocities were determined by changing exhaust pressure with an unchoked exhaust nozzle.

Stability limits were determined by observation of flame extinction through the quartz window in the side of the burner. The stability limit was approached gradually by slowly increasing or decreasing fuel flow. At the instant of blow-out, fuel flow and burner exit total pressure were recorded to permit definition of the stability limits and to compute combustion efficiency at the stability limit. Afterburner air flow (actually air flow plus preheater fuel flow) was determined for a given series of runs from total pressure at the burner exit with no burning and with the exhaust nozzle choked. The exhaust nozzle throat area was known, and an assumed flow coefficient was used in the computation (see appendix A).

The ratio of afterburner exit to inlet temperature was calculated using the ratio of burner exit total pressure with burning to that for nonburning with the nozzle choked, and combustion efficiency was taken as the ratio of actual afterburner temperature rise to the ideal temperature rise at the same fuel-air ratio. The ideal temperature rise was obtained from an ideal temperature rise curve in which dissociation was taken into account (see ref. 8). Computational procedures used in determining afterburner temperature ratio and combustion efficiency are given in appendix A.

Radial fuel-air distribution was checked in several cases at various circumferential positions to within 2 inches of the burner center line and immediately ahead of the flame holder. The fuel-air surveys were made while afterburner combustion was in progress.

The fuel used for this investigation was MIL-F-5624A grade JP-4, which had a heating value of 18,725 Btu per pound and a hydrogen-carbon ratio of 0.172.

RESULTS AND DISCUSSION

Burner Flow Conditions

Inasmuch as the effect of flame-holder gutter shape on combustion performance was of prime interest, it was desirable that all variables pertaining to burner flow conditions be maintained as nearly constant as possible over the entire range of the investigation. In particular, the gas temperature profile, flow velocity profile, and fuel-air distribution were controlled within the limits shown in figures 5 to 8.

Gas temperature. - The gas temperature distribution measured at station 2 ahead of the fuel injection station is shown in figure 5. Three levels of burner inlet velocity are presented in figures 5(a) to (c) for high burner inlet pressure (high air flow) conditions. Except for the lower quadrant, the gas temperatures were within a band of 60° F. At the lowest velocity level, temperatures in all quadrants were within a 60° F band. The radial variations in temperature were similar at all points around the circumference, with a slight lowering of temperature near the outer wall.

In figures 5(d), (e), and (f), the temperature profiles at low pressure are shown for the velocity levels corresponding to those for figures 5(a), (b), and (c), respectively. The pattern was essentially the same as for the high pressure operating conditions except that a maximum deviation in temperature of 200° F occurred at the lowest pressure and velocity (fig. 5(f)).

Burner inlet velocity. - Typical gas velocity profiles at the burner inlet (station 4) surveyed across a horizontal diameter are shown in figure 6 for average burner-inlet velocities of 382, 510, and 675 feet per second. The velocity profile had the same shape for all three velocity levels and is representative of the type found in afterburners used on actual engines. The low velocity core indicated a very thick boundary layer or a partially separated flow region due to the large curvature of the diffuser inner body at the downstream end. As might be expected, the peaks and troughs in the velocity profiles were accentuated at the high velocities.

Fuel-air distribution. - Surveys of fuel-air distribution made at station 4 with the burner operating at inlet velocities between 480 and 520 feet per second are shown in figure 7. Surveys are shown for a fuel-air ratio of 0.050 at a burner inlet pressure of 10.5 inches of mercury

absolute and 0.065 at a burner inlet pressure of 18.5 inches of mercury absolute. Figures 7(a), (b), and (c) show the distribution for these conditions at three positions around the burner circumference designated as degrees of angular position by the convention adopted in figure 4(b). Although some minor nonuniformities in the fuel-air mixture along the radius as well as around the circumference are evident, the patterns are representative of results that could be achieved in the practice of high-output afterburner design. The nonreproducibility of the fuel-air distribution pattern near the center of the burner for the three angular positions may be attributed to the unpredictable eddy and recirculatory flow behind the end of the diffuser inner body.

The fuel-air ratio distributions at a constant air flow rate but with three levels of burner inlet velocity (400, 500, and 650 ft/sec) are shown in figure 8. At the 90° position (fig. 8(a)), the distribution with a velocity of 650 feet per second and a fuel-air ratio of 0.065 was similar to that with a velocity of 400 feet per second and a fuel-air ratio of 0.050.

Visual inspection of the curves in figures 7 and 8 reveals that the average surveyed fuel-air ratio was lower than the over-all fuel-air ratio computed from gross measurements of fuel and air flow. The absolute values of the surveyed fuel-air ratio are therefore doubtful, but they may be considered indicative of the relative fuel-air ratio distribution actually existing along the burner radius.

Typical Performance Characteristics

Except for observed differences in the steadiness of the flame accompanied at times by increase in sound level due to rough burning, there were no outward indications of differences in combustion characteristics from one flame holder to another. A critical comparison of the various flame holders thus necessitated a complete performance evaluation for each gutter shape and exhaust nozzle size, which involved making approximately 1200 runs, followed by cross-plotting of data to determine performance at the same conditions of pressure, velocity, and fuel-air ratio.

A plot of data for the conventional V-gutter flame holder (flame holder 1), which were obtained with the 70 percent exhaust nozzle, is shown in figure 9. These data were arbitrarily selected to show results which are typical of those obtained with a given exhaust nozzle size. The individual curves shown in figure 9 are for constant values of air flow, and the various quantities defining performance are plotted against afterburner fuel-air ratio. (A detailed discussion of the significance of any special combustion variables will be found in appendix A. The symbols used in appendix A and elsewhere in this report are defined in appendix B.)

The combustion efficiency shown in figure 9(a) is comparable with those efficiencies used in references 1 to 3 and 9. As shown in figure 9(a), the value of combustion efficiency at air flows of 16.87 and 21.33 pounds per second was relatively constant between fuel-air ratios of 0.047 and 0.067. The general level of efficiency decreased 20 percentage points as the air flow decreased from 21.33 to 8.20 pounds per second; there was an attendant decrease in burner inlet pressure from about 16 to 6.5 inches of mercury absolute for this change in air flow rate, as shown in figure 9(b). The fuel-air ratio for peak efficiency, at fuel-air ratios leaner than stoichiometric, generally shifted from about 0.047 to 0.057 as the burner inlet pressure decreased from 16 to 6.5 inches of mercury absolute. As fuel-air ratio was varied at a constant air flow, there was a simultaneous change in both burner inlet pressure and velocity, as shown in figures 9(b) and (c), respectively.

The computed values of combustion efficiency at lean or rich blow-out were somewhat sporadic. Although the data were obtained under transient conditions the primary variable, afterburner fuel flow, was being changed very slowly at the time of blow-out. Generally, however, blow-out was preceded by appreciable instability and flickering of the combustion zone. This flame instability near blow-out was considered to be a factor contributing to the sporadic deviations of combustion efficiency.

The stability limits are defined as the combination of afterburner fuel-air ratio, combustion-chamber pressure, and burner inlet velocity at blow-out and are shown as the dark end points in figure 9. As the burner outlet pressure (fig. 9(d)) decreased from 12.6 inches of mercury absolute to 5.4 inches of mercury absolute, the lean blow-out fuel-air ratio increased from 0.03 to 0.06. At pressure levels of 12 and 15.5 inches of mercury absolute, rich blow-out was not encountered at fuel-air ratios slightly greater than 0.08. The low pressure at which the lean and the rich limit converged indicated the pressure below which flame would not stabilize at any fuel-air ratio for the burner inlet velocities which existed.

A factor which contributed to narrowing the stability limits was the combining effect of velocity, pressure, and fuel-air ratio near blow-out. With a fixed-area choked exhaust nozzle, the burner inlet velocity was a function of the temperature ratio across the burner. At a given air flow, as fuel-air ratio approached blow-out, a drop in efficiency, or temperature ratio, caused a drop in pressure and an increase in velocity. Both factors were changing in the direction of unstable combustion and precipitated blow-out.

The combustion temperature T_5 plotted in figure 9(e) is the overall bulk temperature of a hypothetical gas mixture which would give rise to a particular total pressure upstream of a choked station having a known area and discharge coefficient. The peak in temperatures for the

conditions investigated occurred between fuel-air ratios of 0.060 and 0.072. The maximum temperature of 3740° F obtained for this configuration occurred at a fuel-air ratio of 0.072 and a burner inlet pressure of 16.7 inches of mercury absolute. The combustion temperature at peak efficiency for this pressure level was 3360° R at 0.045 fuel-air ratio.

The broken curve in figure 9(e) indicates the ideal temperature curve which might be obtained with 100 percent combustion efficiency. The flattening of the experimental temperature curve near stoichiometric fuel-air ratio caused a more pronounced departure from the ideal than at other fuel-air ratios and resulted in the dip in the efficiency curve of figure 9(a). This accentuated departure from the ideal curve may be due to combined effects of nonuniformities in the fuel-air ratio distribution and the presence of preheater combustion products. It is also possible that the assumptions regarding the effect of dissociation on ideal combustion temperature rise were not entirely correct, and that the ideal curve should in reality be more flat in the region of stoichiometric fuel-air ratio than is shown.

The ratio of total-pressure loss across the flame holder and the burner to the burner inlet pressure is shown in figure 9(f) for both nonburning and burning conditions. In the nonburning case the pressure loss was due to friction and turbulence and is designated drag. This loss varied from 0.020 to 0.043 times the inlet total pressure with the greater loss occurring at the high air flows (or, inasmuch as the velocity was approximately constant, at high Reynolds numbers). (The present investigation covered a Reynolds number range from 9000 to 25,000.)

The pressure loss with burning ranged from approximately 0.045 to 0.075 times the inlet pressure, and at a given fuel-air ratio it varied with inlet air flow in a manner similar to that found in the case of nonburning. The pressure loss with burning was the sum of the drag and the momentum losses resulting from the heating and accelerating of the gases in a constant-diameter duct. As combustion temperature increased, the pressure loss first increased and then approached a nearly constant value.

Effect of Flame-Holder Gutter Shape on Combustion Efficiency

The combustion performance of a typical flame holder was presented in the previous section as a function of afterburner fuel-air ratio. Similar plots of performance data from other flame holders showed the same general characteristics. Cross plots of the performance data, such as that shown in figure 9, were made at constant values of afterburner fuel-air ratio in order to determine the effects of flame-holder gutter shape on combustion efficiency.

The effect of burner inlet pressure on combustion efficiency at the three main velocity levels for the various flame-holder shapes is shown in figure 10 for a fuel-air ratio of 0.047, and in figure 11 for a fuel-air ratio of 0.067. The data shown in each part of figures 10 and 11 are for a fixed exhaust nozzle throat size, and the burner inlet velocity, as a result, varied slightly with combustion efficiency. As can be seen in these figures, the variation of combustion efficiency with burner inlet pressure at both fuel-air ratios was generally the same for all flame-holder shapes. The combustion efficiency decreased with decreasing burner pressure, and the rate of decrease in combustion efficiency increased with increasing burner inlet velocity. A peculiarity in the behavior of combustion efficiency with burner inlet pressure can be observed for the lowest velocity levels (figs. 10(a) and 11(a)). Above pressures of approximately 15 inches of mercury absolute, the efficiency appeared to decrease slightly with increasing pressure. The reasons for this apparent decrease in combustion efficiency with increasing pressure are unknown.

The effect of velocity on combustion efficiency for the various flame-holder shapes is shown in figures 12 and 13 for fuel-air ratios of 0.047 and 0.067, respectively. The trend of combustion efficiency with increasing velocity was again similar for all flame-holder shapes. The combustion efficiency decreased with increasing velocity at a rate which was primarily dependent upon the pressure level in the burner. For a fuel-air ratio of 0.047 an increase in velocity from 400 to 600 feet per second was accompanied by about 7 percentage points loss in efficiency at a burner inlet pressure of 15 inches of mercury absolute (fig. 12(a)). At 8 inches of mercury absolute (fig. 12(c)), the same increment of velocity increase caused a loss of about 15 percentage points in efficiency. Similar interrelated effects of pressure and velocity were found at a fuel-air ratio of 0.067, as shown in figure 13.

As shown in figures 10 to 13, the over-all variation in combustion efficiency was from about 90 percent at a velocity of 400 feet per second and a pressure of 15 inches of mercury to about 60 percent at a velocity of 700 feet per second and a pressure of 8 inches of mercury. Although within the over-all range of combustion efficiency variation the trend of combustion efficiency with either increasing velocity or decreasing pressure was similar for all flame-holder shapes, the performance of each of the various flame-holder shapes at given conditions of velocity, pressure, and fuel-air ratio was not exactly the same. At given conditions of operation, differences of 5 to 10 percentage points for the various flame-holder shapes were observed. Because the differences in combustion efficiency were not consistent, however, a more detailed examination of the data was necessary in order to isolate the actual magnitude of effect of flame-holder shape on combustion efficiency.

Although normal inaccuracies in combustion efficiency due to experimental error are as much as 5 to 10 percentage points, they may be assumed to be largely random in nature. Averaging a large number of data points might, therefore, bring out any trends due to flame-holder shape, even though small and obscured by data scatter. To accomplish this averaging treatment, differences at identical conditions of fuel-air ratio and pressure between the combustion efficiency obtained with the conventional V-gutter (flame holder 1) and that obtained with each of the other flame-holder shapes were determined from plots similar to those in figure 9. Combinations of fuel-air ratio and pressure were arbitrarily preselected to give a wide range of conditions and a large number of averaging points for each flame holder. The differences in efficiency obtained were then averaged arithmetically to determine the merit of a given flame holder relative to the conventional V-gutter.

The results of this averaging process are shown in bar-graph form in figure 14. The average differences in efficiency are arranged where possible in order of increasing K/V , a vortex-strength parameter which was found in the isothermal investigation of reference 6 to be characteristic of a given flame-holder shape. Also shown in figure 14 is the total number of experimental runs made for each flame holder.

For the first seven flame-holder shapes shown in figure 14, there is no evidence of any functional relation between the combustion efficiency and the vortex-strength parameter. The results do, however, show some differences in combustion efficiency between the various flame-holder shapes. The U-shaped gutter (flame holder 10) has a combustion efficiency approximately 7 percentage points poorer than that for the conventional V-flame holder, a result in qualitative agreement with other experiments reported in reference 10. A flame holder with vortex generators near the downstream edge of the legs of the "V" (flame holder 8) had an average combustion efficiency which was 3.5 percentage points better than the conventional V, and three other flame holders had efficiencies ranging from 1.5 to 2.0 percentage points better.

Thus, the over-all difference in combustion efficiency due to flame-holder shape was 10 percentage points. The maximum improvement in combustion efficiency over the conventional V-gutter flame holder was only 3.5 percentage points, however. All four flame holders (5 to 8) which had more than 1 percentage point superiority over the conventional V-gutter flame holder had slightly higher pressure drops, as will be discussed in more detail, and these characteristics as well as relative difficulty of manufacture would have to be considered when choosing a flame-holder shape for practical application.

Effect of Flame-Holder Gutter Shape on Pressure Loss

The pressure loss across a body in a moving gas stream is indicative of the change in momentum of the gas in the direction of the flow, or the drag force incurred upon the body. In the case of nonburning, the momentum change in the gas stream is the difference in momentum between the undisturbed free stream and the wake region behind the gutters. The pressure loss without burning is an important consideration in afterburner design primarily because of its effect on economy of engine operation in cruising flight. In the case of burning, the losses consist of not only the flame-holder drag but also the loss in momentum due to the acceleration of heated gases in a constant-diameter duct. Losses in this case would be a function of the combustion-chamber inlet conditions (Mach number and pressure) and the temperature ratio across the burner. Pressure losses with burning are important because of the direct effect on maximum output obtainable from an afterburner, and also, in some cases where supersonic flight plans call for a cruise with afterburning, because of the effect on over-all economy of engine operation.

Losses without burning. - The ratio of the loss in total pressure across various flame-holder gutters with no burning to the total pressure upstream of the gutters is shown in figure 15 as a function of inlet velocity. Up to velocities of 400 feet per second, losses for all the gutter shapes were 1 percent or less of the upstream pressure. At 650 feet per second, the losses varied from 1 to 3 percent of the upstream pressure.

The smallest losses were exhibited by the conventional V-gutter flame holder (1) and the U-shaped flame holder (10). Flattening the upstream face of the U-shaped gutter and adding sharp-edged tabs to the trailing edges of the V-gutter gave flame holders (2 and 3) with the highest pressure losses. Cambering the walls of the V-gutter or adding vortex generators both upstream and at the trailing edge of the gutter legs, or adding semicircular tabs to the trailing edge gave flame holders (5 to 8) with intermediate pressure drops. These flame holders, which had a pressure drop approximately 1 percentage point higher than for the conventional V-gutter at a velocity of 650 feet per second, were previously shown to have a slight superiority over the conventional V-gutter with respect to combustion efficiency.

Losses with burning. - Figure 16 shows the pressure loss ratio with burning for five gutter shapes at burner inlet velocities of 500 and 600 feet per second as a function of burner temperature ratio. At a burner inlet velocity of 500 feet per second, as shown in figure 16(a), the differences in pressure loss ratio for the conventional V-gutter flame holder, the cambered V-gutter flame holder, and the flame holder with upstream vortex generators were similar over the entire range of temperature ratio. The flame holders with the flattened upstream face and the sharp tabs at the trailing edge had the highest losses, as was the case with no burning.

At a burner inlet velocity of 600 feet per second (fig. 16(b)), the trends of pressure loss ratio with both temperature ratio and flame-holder shape were similar to the trends obtained at a burner inlet velocity of 500 feet per second. The increase in velocity from 500 to 600 feet per second increased the pressure loss ratio by 2 to 4 percentage points.

Effect of Flame-Holder Gutter Shape on Stability Limits

As explained in a previous section, combustion stability limit is the combination of flow variables and fuel-air ratio at which flame can no longer be stabilized and propagated into the main stream. A typical set of blow-out data is shown in figure 17 where the fuel-air ratio and burner pressure at the instant of blow-out are plotted for the conventional V-gutter flame holder. Data are shown for the three exhaust-nozzle sizes. The locus of blow-out points defines the stability limit, which in figure 17 covered a wide range of burner inlet velocities. The numbers beside each blow-out point indicate the velocities at time of blow-out computed as a function of the burner temperature ratio.

A cross plot at constant burner inlet velocities of the aforementioned blow-out data for the conventional V-gutter flame holder is shown in figure 18. Only limited data were obtained at a velocity of 700 feet per second and as a result the rich limit is not shown for this velocity. The variation of stability limits with combustion-chamber pressure for the conventional V-gutter flame holder was typical of stability limits of the other flame-holder gutter shapes. As combustion-chamber pressure decreased, the fuel-air ratio at which blow-out occurred changed slowly until a pressure of about 7 inches of mercury was reached. Below 7 inches of mercury the stability limits were very sensitive to pressure. The lean and rich limits converged rapidly until, at some minimum pressure, flame would not stabilize at any fuel-air ratio for a given burner inlet velocity. This minimum pressure for flame stabilization, which was dependent upon the burner inlet velocity, was not determined for all flame-holder gutter shapes.

A comparison of stability limits for a selection of four flame-holder gutter shapes at a burner inlet velocity of 500 feet per second is shown in figure 19. The limits of all shapes for which data were sufficiently complete grouped within a fuel-air ratio of 0.01 except at very low pressures. The flame holder with sharp-edged tabs was slightly poorer than the others at the rich limit, and the flame holder with upstream vortex generators was poorer at the lean limit.

Stability limits for the same gutter shapes at a velocity of 600 feet per second are shown in figure 20. In general, the limits were narrower than those at 500 feet per second by 0.003 to 0.005 in fuel-air ratio. The flame holder with the upstream vortex generators again

exhibited poorer lean limits, which may be due to the presence of turbulence upstream of the flame stabilizer. Similar effects of upstream turbulence on stability limits were reported in reference 5, where increasing turbulence intensity decreased the stability limits.

The relative insensitivity of stability limits to the gutter shapes investigated may be due to the behavior of wake flow characteristics and to the dynamics of gas flow at blow-out. Changes in flow characteristics in the region immediately behind the gutter from those observed during isothermal flow occur as a result of seating flame on the gutter. With combustion and expansion of gases occurring, the large differences in wake flow behind gutters of various shapes found during isothermal flow (ref. 6) might be reduced during burning to a small recirculating type of flow that is similar for all gutter shapes.

Another factor contributing to the similarity of stability limits for the various shapes might be the dynamics of flow and the coupling of flow variables at impending blow-out. Should the blow-out process initiate by inability of flame to propagate into the main stream, as observed and found to be independent of gutter shape in reference 5, the greater portion of the combustion reaction normally occurring in the burner would cease. In a chamber with a choked exit, a drop in combustion temperature due to cessation of the main portion of the combustion reaction would result in a sudden drop in chamber pressure. The rapid pressure change followed by a sudden acceleration of the approaching fuel-air mixture could give rise to conditions at which even the flame stabilizing source is extinguished despite favorable conditions that might be created in the wake region by some particular flame-holder gutter shape. In a combustion-chamber system with a choked exit, the factor controlling stability limits may then become the stability limits of the flame propagation process, which might be quite independent of the effects of gutter shape and of the mechanics of flame stabilization in the wake of bluff bodies.

CONCLUDING REMARKS

An investigation was conducted in a 26-inch-diameter afterburner test rig to determine the effect of flame-holder gutter cross-sectional shape on afterburner performance. The flame-holder shapes investigated included a conventional V-gutter, a cambered V-gutter, and V-gutters modified by the addition of trailing-edge tabs or vortex generators both upstream and at the trailing edges. Also included were channel-shaped gutters with both rounded and flattened upstream faces.

The investigation covered burner inlet velocities ranging from 380 to 700 feet per second and burner pressures ranging from 6 to 20 inches of mercury absolute. Combustion efficiencies of about 90 percent were

obtained at a burner inlet velocity of 400 feet per second and a burner pressure of 15 inches of mercury absolute. At a burner inlet velocity of 700 feet per second and a burner pressure of 8 inches of mercury, combustion efficiencies of 60 percent were obtained.

The effect of increasing burner inlet velocity and decreasing burner inlet pressure on combustion efficiency was about the same for all flame-holder shapes. At given operating conditions no trend of combustion efficiency with flame-holder shape could be isolated and shown to be consistent with the trend at other conditions; data scatter due to random experimental error concealed any effects present. A process which involved averaging a large number of differences in combustion efficiency did, however, reveal some effects of flame-holder shape on combustion efficiency. By this averaging process a channel-shaped gutter with a rounded upstream face was found to give a combustion efficiency 7 percentage points poorer than that of a conventional V-gutter. Addition of vortex generators to the trailing edge of a conventional V-gutter improved the combustion efficiency by 3.5 percentage points. Thus, an over-all variation in combustion efficiency due to flame-holder shape of 10 percentage points was found. The maximum improvement in combustion efficiency over that for a conventional V-gutter flame holder was only 3.5 percentage points, however.

The conventional V-gutter flame holder was among those flame-holder shapes giving the lowest pressure drop both with and without burning in the combustion chamber. At a velocity of 500 feet per second the pressure drop for a channel flame holder with a flat upstream face and a V-gutter with sharp-edged trailing-edge tabs, the poorest flame holders with regard to pressure drop, gave pressure drops which were 1 percentage point higher than the conventional V-gutter. With burning, the differences in pressure drop between the conventional V-gutter and these flame holders were from 2 to 4 percentage points.

Flame-holder shape had a small effect on stability limits. Turbulence created by the addition of vortex generators upstream of a conventional V-gutter appeared to have a slight adverse effect on the lean limit of combustion.

Lewis Flight Propulsion Laboratory
National Advisory Committee for Aeronautics
Cleveland, Ohio, October 12, 1953

METHODS OF CALCULATION

Gas flow. - The gas flow through the nozzle for a given series of runs was computed as

$$W_{g6} = \frac{C_d P_5 A_6}{\sqrt{RT_5}} \sqrt{(\gamma g) \left(\frac{2}{\gamma + 1} \right)^{\frac{\gamma+1}{\gamma-1}}}$$

The gas flow was computed for the cold flow condition (only preheater lit, $T_5 = 1250^\circ \text{ F}$) and this flow was assumed to remain constant during all corresponding hot runs (afterburner lit) at the same setting of the inlet-air supply valve.

Air flow. - The weight of air flow through the afterburner was computed as

$$W_a = W_g - W_{f_p}$$

Burner inlet velocity. - The continuity equation was used in the following form to calculate the afterburner inlet velocity from measurements of total pressure, static pressure, and area made at station 4 and of afterburner inlet temperature made at station 2:

$$V_4 = \frac{(W_g + W_{f_b}) RT_2}{A_4 P_4} (P_4/P_2)^{\frac{\gamma-1}{\gamma}}$$

Fuel-air ratio. - Three significant fuel-air ratios used in this report were defined as follows:

$$(f/a) = \frac{W_{f_p} + W_{f_b}}{W_a} \text{ (over-all)}$$

$$(f/a)_p = W_{f_p}/W_a \text{ (preheater)}$$

$$(f/a)_a = \text{afterburner unburned-air}$$

The method of obtaining $(f/a)_a$ is as follows:

$$(f/a)_a = \frac{\text{total unburned fuel to afterburner}}{\text{total unburned air}} = \frac{W_{f_b} + (W_{f_p} - W_{f_p}')}{\left(W_a - \frac{W_{f_p}'}{(f/a)_{\text{stoich}}} \right)}$$

where

$(W_{f_p} - W_{f_p}')$ = fuel not burned in preheater to be charged to afterburner

$\left(\frac{W_{f_p}'}{(f/a)_{\text{stoich}}} \right)$ = air theoretically chemically consumed in preheater

Dividing by W_a yields

$$(f/a)_a = \frac{(f/a)_b + (f/a)_p - (f/a)_p'}{1 - \frac{(f/a)_p'}{0.0675}}$$

but

$$(f/a)_b + (f/a)_p = (f/a)$$

therefore,

$$(f/a)_a = \frac{(f/a) - (f/a)_p'}{1 - \frac{(f/a)_p'}{0.0675}}$$

The value of $(f/a)_p'$ is obtained from the ideal temperature rise curve (ref. 8) and measurements of the burner inlet total temperature and the inlet air supply temperature upstream of the preheater ($77 \pm 3^\circ \text{ F}$).

Total temperature across burner. - The burner total temperature ratio was derived from the continuity equation applied at the choked nozzle throat and is defined as

$$\sqrt{T_{5_h}/T_{5_c}} = \left(\frac{1 + (f/a)_p}{1 + (f/a)} \right) P_{5_h}/P_{5_c} \sqrt{\frac{\gamma_h R_c}{\gamma_c R_h} \frac{\left(\frac{\gamma_c + 1}{2} \right)^{\frac{\gamma_c + 1}{2(\gamma_c - 1)}}}{\frac{\gamma_h + 1}{2(\gamma_h - 1)}} \frac{\gamma_h + 1}{\left(\frac{\gamma_h + 1}{2} \right)^{\frac{\gamma_h + 1}{2(\gamma_h - 1)}}}}$$

Air flow W_a was set and assumed constant for hot and cold cases.

Afterburner combustion efficiency. - The afterburner combustion efficiency used in this report is defined as follows:

$$\eta = \frac{T_{5_h} - T_2}{T_{5_h}' - T_2}$$

where T_{5_h}' is the ideal combustion temperature determined from the actual over-all fuel-air ratio (f/a) and the ideal temperature rise curve of reference 8.

The significance of this combustion efficiency is indicated in figure 21. The ideal combustion temperature T_{5_h}' calculated with the use of reference 8, which takes into account the effect of dissociation, is shown as a broken curve. The experimental points shown are typical of those obtained in the flame-holder investigation. The combustion efficiency at any experimental fuel-air ratio is the ratio of actual to ideal rise in temperature above the inlet gas temperature T_2 . A combustion efficiency defined in this manner evaluates, on the basis of an ideal combustor, the effectiveness of the afterburner combustion process in creating a temperature increase. The proximity with which the actual combustion temperature approaches the ideal temperature at any given fuel-air ratio is thus a measure of combustion efficiency.

Although this combustion efficiency evaluates how closely the burner approaches ideal combustion, it does not adequately show the expenditure of fuel in obtaining an increment of temperature increase. Referring again to figure 21, in the region of lean fuel-air ratio the increment of fuel needed to obtain a 100° rise in combustion temperature is represented by Δf_a . In the region of rich fuel-air ratio near stoichiometric, a much larger quantity of fuel represented by Δf_b is required to obtain the same 100° rise in temperature.

It is also evident that if the actual combustion temperature curve is everywhere equal in slope to the ideal curve but displaced a finite distance along the ordinate, the combustion efficiency will never be 100 percent. The increment of fuel required to obtain a given increment of temperature rise, however, will be no greater than in the ideal case.

The combustion efficiency discussed is plotted in figure 22. Also shown in this figure for comparison is the efficiency for the same data computed by the method given in reference 9, in which combustion efficiency was defined as the ratio of the energy increase in the afterburner to the ideal energy increase obtainable from the same quantity of fuel. The agreement between the two methods was within 3 percent over the entire range of afterburner fuel-air ratio.

SYMBOLS

The following symbols are used in this report:

A	area, sq ft
C_d	discharge coefficient
(f/a)	over-all fuel-air ratio
(f/a) _a	afterburner unburned-air fuel-air ratio
(f/a) _p	preheater fuel-air ratio
g	acceleration due to gravity, 32.174 ft/sec ²
K	vortex strength, ft ² /sec
P	total pressure, lb/sq ft abs or in. Hg abs
p	static pressure, lb/sq ft abs or in. Hg abs
R	gas constant, 53.3 ft-lb/(°R)
T	total temperature, °R or °F
V	velocity, ft/sec
W _a	air flow, lb/sec
W _f	fuel flow, lb/sec
W _g	gas flow, lb/sec
γ	ratio of specific heats
η	combustion efficiency

Subscripts:

b	afterburner
c	cold flow condition, only preheater operative

- h hot flow condition, preheater and afterburner operative
- p preheater
- 2 before spray bars
- 4 burner inlet (diffuser outlet)
- 5 burner exit (nozzle inlet)
- 6 exhaust-nozzle throat

Superscript:

- ' indicates ideal case

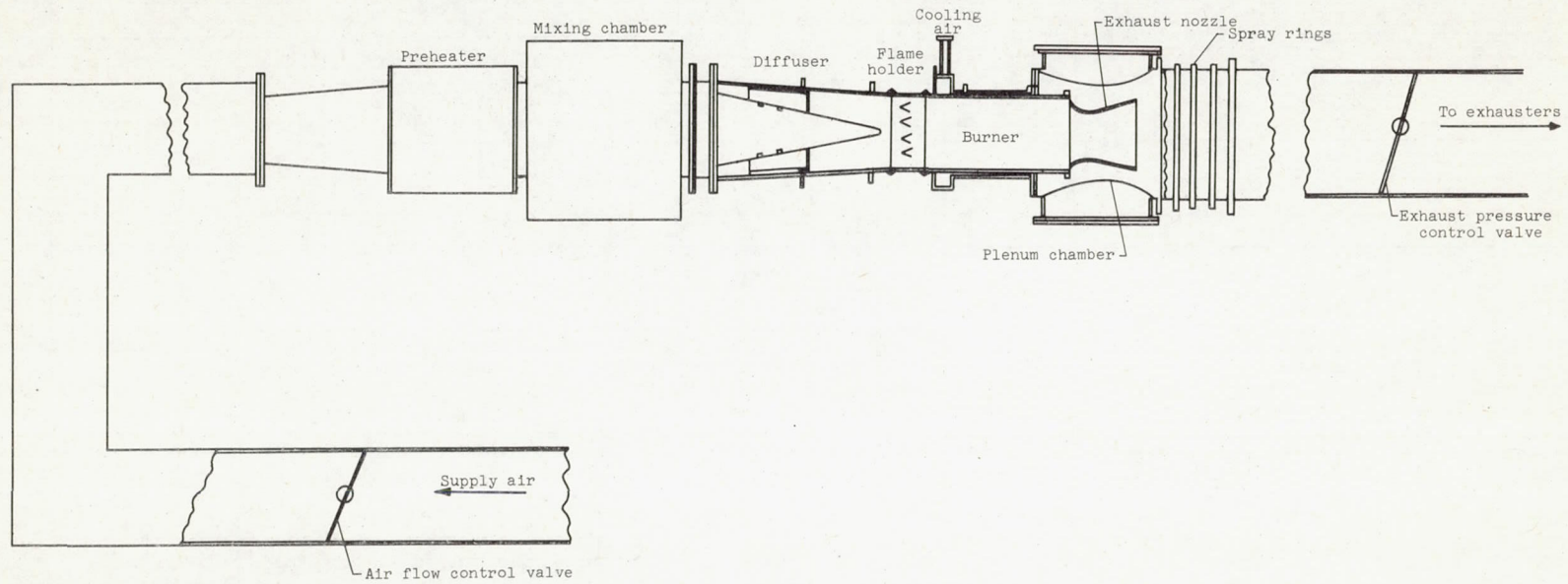
REFERENCES

1. Huntley, S. C., and Wilsted, H. D.: Altitude Performance Investigation of Two Flame-Holder and Fuel-System Configurations in Short Afterburner. NACA RM E52B25, 1952.
2. Conrad, E. William, and Campbell, Carl E.: Altitude Wind Tunnel Investigation of High-Temperature Afterburners. NACA RM E51L07, 1952.
3. Braithwaite, Willis M., Renas, Paul E., and Jansen, Emmert T.: Altitude Investigation of Three Flame-Holder and Fuel-Systems Configurations in a Short Converging Afterburner on a Turbojet Engine. NACA RM E52G29, 1952.
4. Longwell, J. P., Chenevey, J. E., Clark, W. W., and Frost, E. E.: Flame Stabilization by Baffles in a High Velocity Gas Stream. Third Symposium on Combustion, Flame, and Explosion Phenomena, The Williams & Wilkins Co. (Baltimore), 1949, pp. 40-44.
5. Scurlock, A. C.: Flame Stabilization and Propagation in High-Velocity Gas Streams. Meteor Rep. No. 19, M.I.T., May 1948. (Contract NOrd 9661.)
6. Younger, George G., Gabriel, David S., and Mickelson, William R.: Experimental Study of Isothermal Wake-Flow Characteristics of Various Flame-Holder Shapes. NACA RM E51K07, 1952.
7. Gerrish, Harold C., and Meem, J. Lawrence, Jr.: The Measurement of Fuel-Air Ratio by Analysis of the Oxidized Exhaust Gas. NACA Rep. 757, 1943. (Supersedes NACA WR E-128.)

8. Mulready, Richard C.: The Ideal Temperature Rise Due to the Constant Pressure Combustion of Hydrocarbon Fuels. M.I.T., Meteor Rep. UAC-9, Res. Dept., United Aircraft Corp., July 1947. (BuOrd Contract NOrd 9845.)
9. Useller, James W., Harp, James L., Jr., and Fenn, David B.: Turbojet-Engine Thrust Augmentation at Altitude by Combined Ammonia Injection into the Compressor Inlet and Afterburning. NACA RM E52L19, 1953.
10. Renas, Paul E., and Jansen, Emmert T.: Effect of Flame-Holder Design on Altitude Performance of Louvered-Liner Afterburner. NACA RM E53H15, 1953.

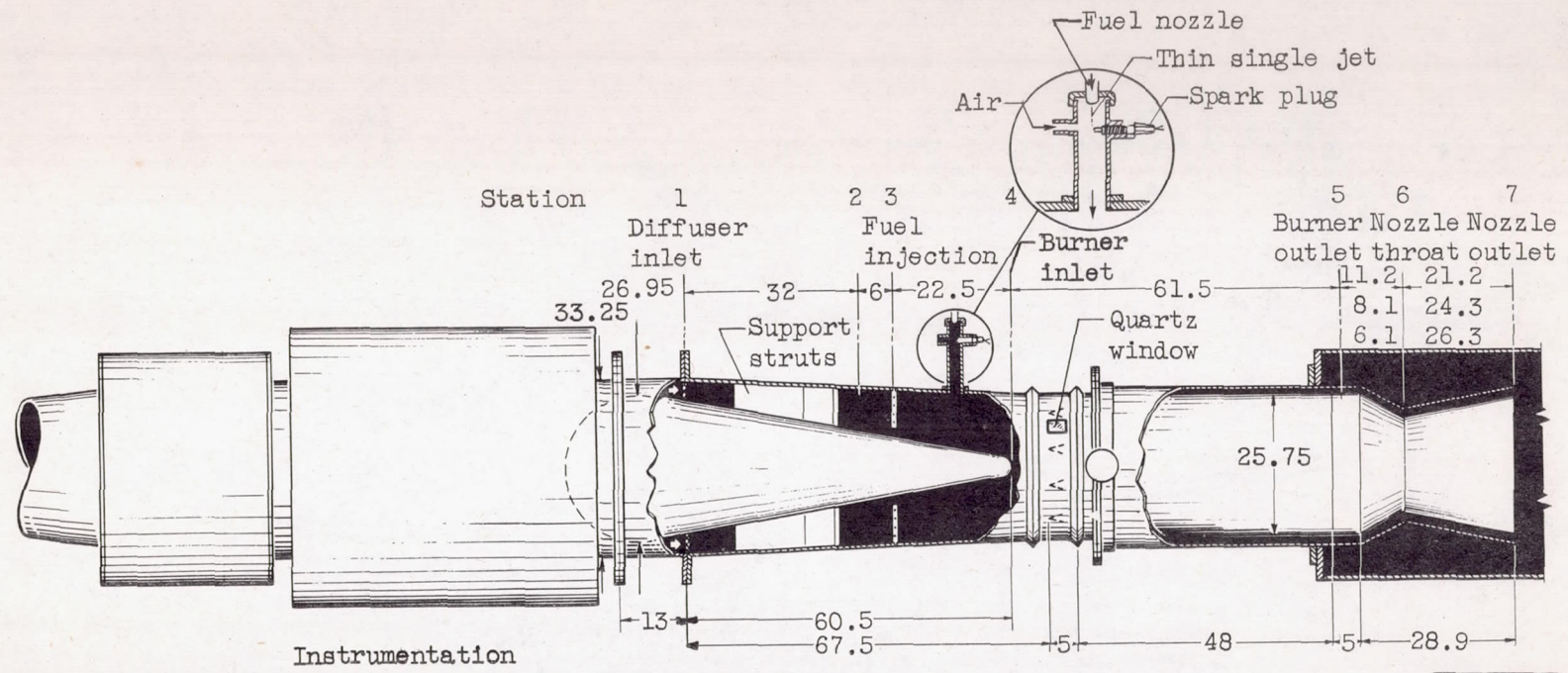
TABLE I. - PERFORMANCE VARIABLES

Flame holder	Flame-holder gutter shape	Nozzle size, A_6/A_5	Burner inlet velocity, V_4 , ft/sec	Air flow, lb/sec								Burner inlet pressure, in. Hg abs (average for air flow level)									
				a	b	c	d	e	f	g	h	a	b	c	d	e	f	g	h		
1	V	0.522	380-450	6.5	7.68	9	10.8	13	16	20			5.7	7	8.6	10	12	15	18.5		
		.70	500-600	8.2	9.3	10.2	11	11.9	16.9	21.3			5.8	6.6	7.3	8	9	12.5	15.4		
		.82	580-700	13	14.5	16.5	20	24.8					7.8	8.6	10.3	12.4	13.9				
2	□	0.522	380-450	11.2	13.3	16.3	20						10.8	12	15	18.5					
		.70	500-600	10	11.2	12.1	14.5	17.6	21.8				7.2	8.0	9.6	10.2	12.7	15.6			
		.82	580-650	13.4	15.5	18.6	23						8.3	10.2	12.3	15.3					
3	∩	0.522	380-450	6.5	7.5	9.2	10.8	13	16.2	20			5.7	7	8.6	10	12	15	18.5		
		.70	500-600	12.4	14.1	17.4	21.6						9.8	10.1	12.6	15.5					
		.82	580-670	12	14	15.9	19.1	23.8					7.5	8.6	10.2	12.5	15.5				
4	∩	0.522	380-450	11	13	16							10.8	12	15						
		.70	500-600	10.8	12.8	15	16	17.7	21.4	27.7			7.6	9.8	11	12	13	15.4	20.9		
5	∩	0.522	380-450	6.3	7.6	9	11.5	13	16	20			5.7	7	8.6	11	12	15	18.5		
		.70	500-600	8.1	8.9	10	11	12	14.3	17.7	22.1			5.8	6.6	7.2	7.9	9.6	10.1	12.8	15.6
		.82	580-700	12.5	14.1	19.4	25.1						7.7	8.6	12.5	16					
6	∩	0.522	380-450	7.3	9	10.8	12.9	16.2					7	8.6	10	12	15				
		.70	500-600	8.7	9.7	10.3	12	17.7	21.44				6.1	7.1	7.4	9.6	12.8	15.5			
		.82	580-700	14.1	16.8	19.9	24.9						8.6	10.4	12.6	15.9					
7	∩	0.70	500-600	12.3	14.5	17.4	21.7					9.7	10.5	12.6	15.5						
8	∩	0.522	380-450	7.8	10.6	15.8						7	10	15							
9	∩	0.522	380-450	7.7	9.2	11.7	16	20					7	8.6	11	15	18.5				
		.70	500-600	8	9	10	11	11.7	15	17.7	21.4		5.8	6.6	7.2	7.9	8.9	11	12.8	15.4	
10	∩	0.70	500-600	9.9	10.8	13	16.7	21.5				7.1	7.8	9.8	12.2	15.4					



(a) General arrangement.

Figure 1. - Schematic layout of simulated afterburner test rig.



CD-3399

^a Station	Total-pressure tubes	Static-pressure tubes	Wall static orifices	Thermo-couples
2	--	-	-	25
4	26	4	8	--
5	12	-	2	--
7	--	-	1	--

^aInstrumentation at stations 1, 3, and 6 not used in computation.

(b) Burner details. (Dimensions are in inches.)

Figure 1. - Schematic layout of simulated afterburner test rig.

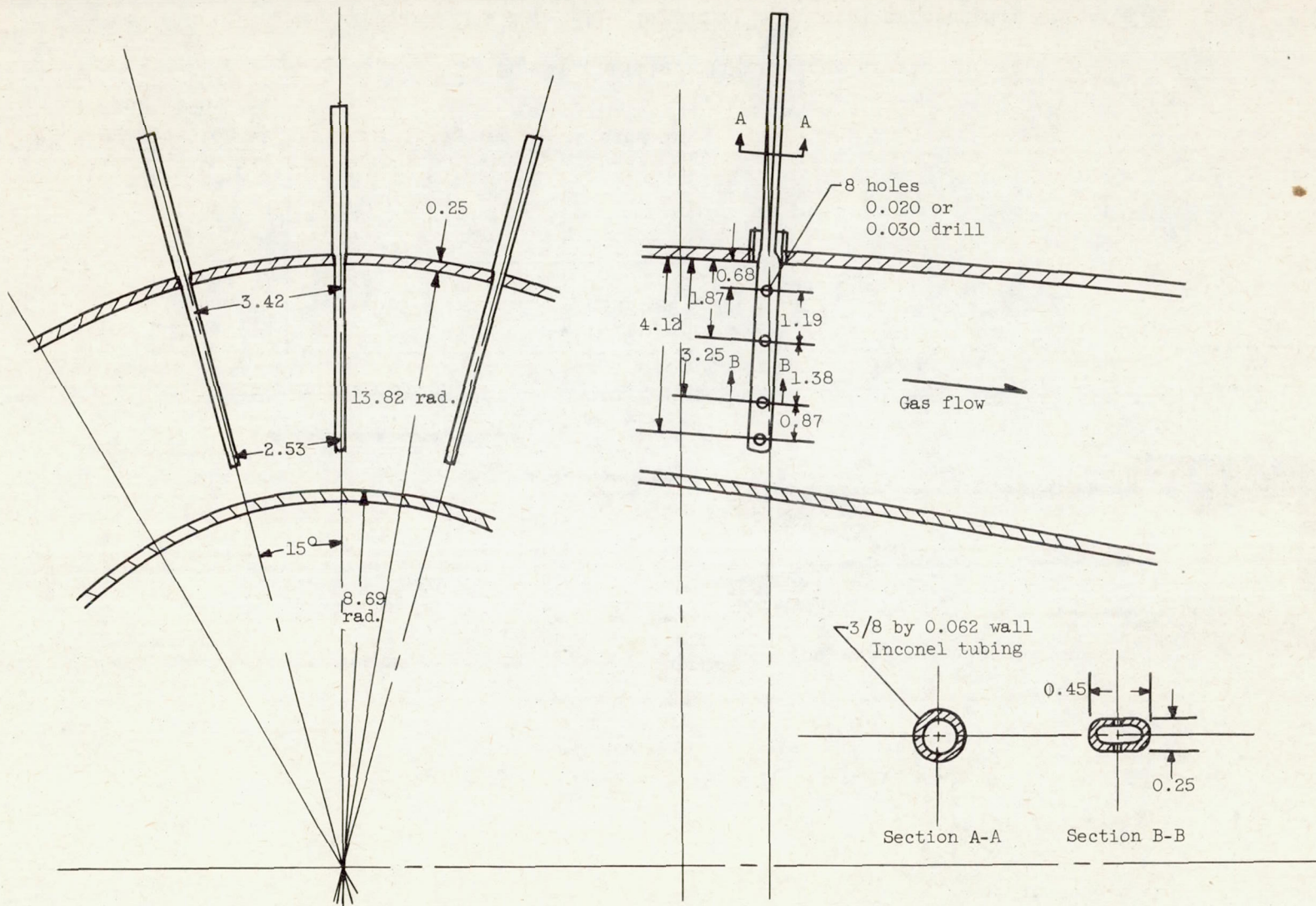
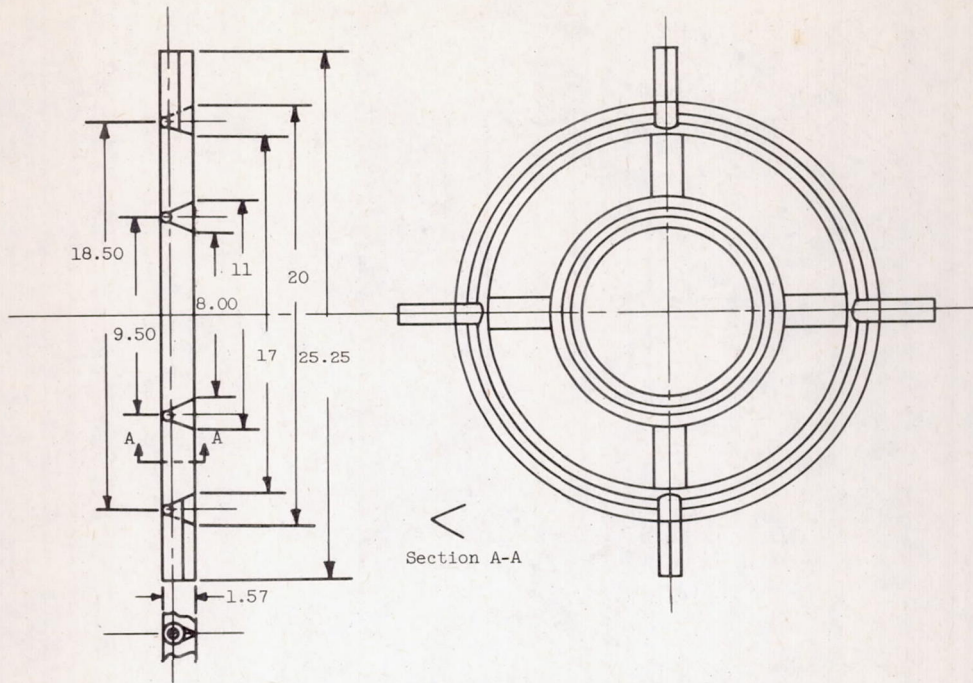
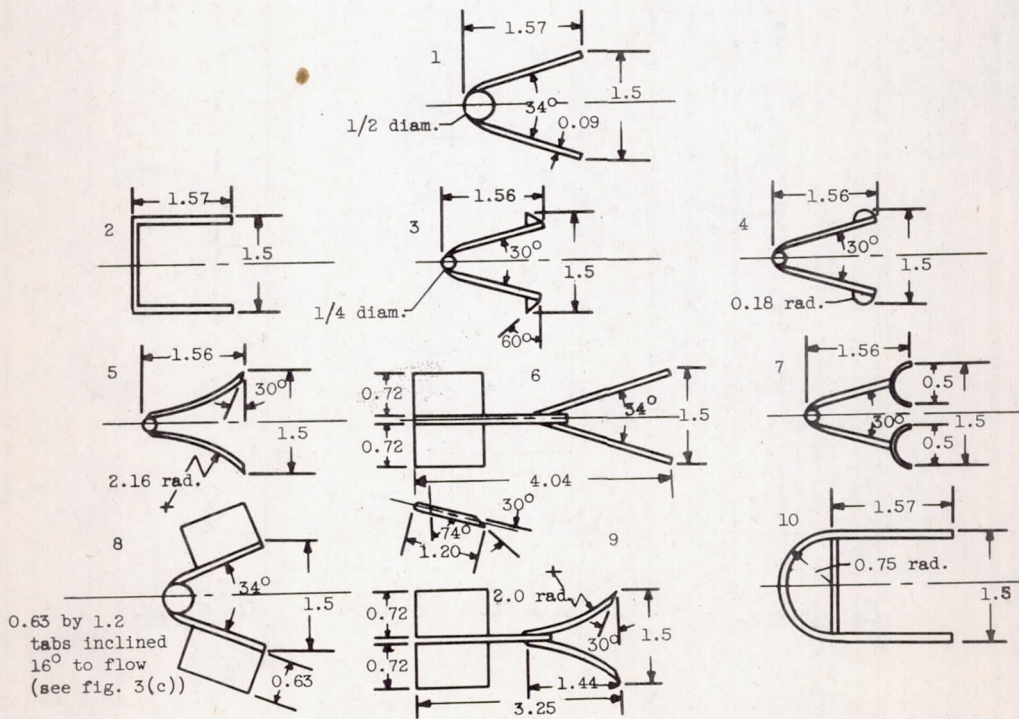


Figure 2. - Afterburner fuel injection system. (Dimensions are in inches.)



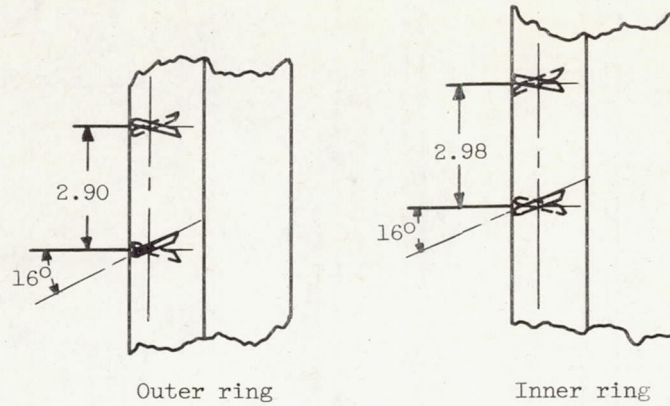
(a) General dimensions of typical flame-holder.



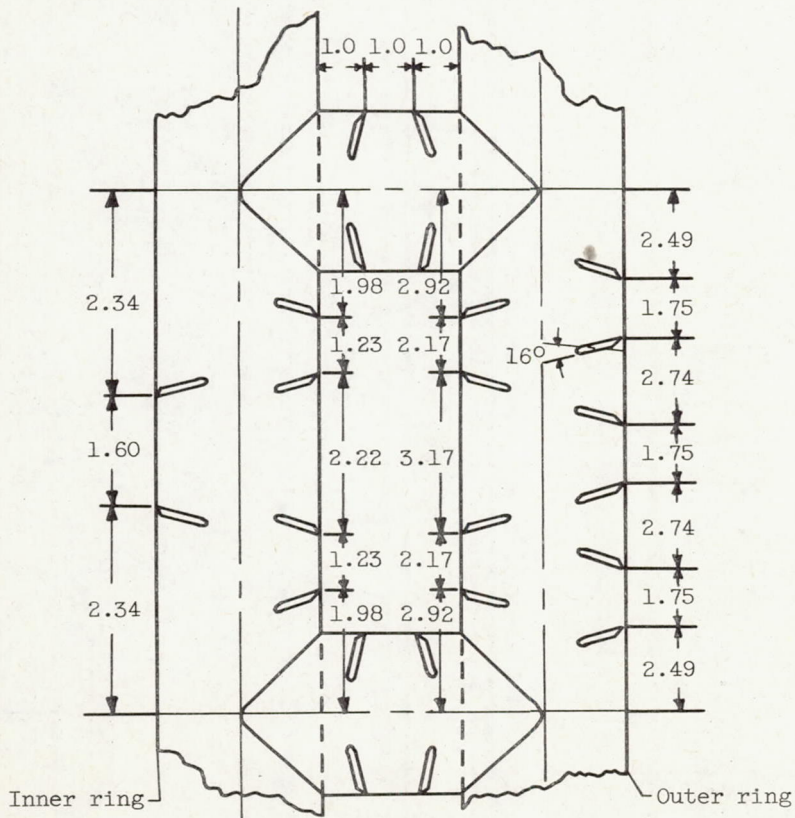
(b) Cross sections of flame-holder gutter shapes.

Figure 3. - Flame-holder geometry. (Dimensions are in inches.)

Flame holders 6 and 9

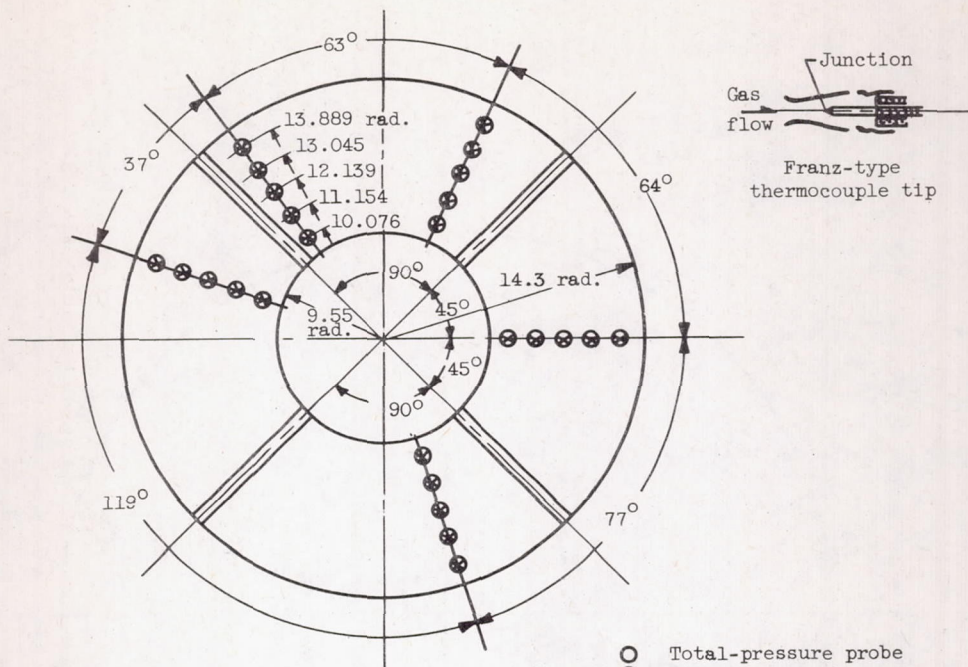


Flame holder 8; developed view of flame holder shown in flattened position

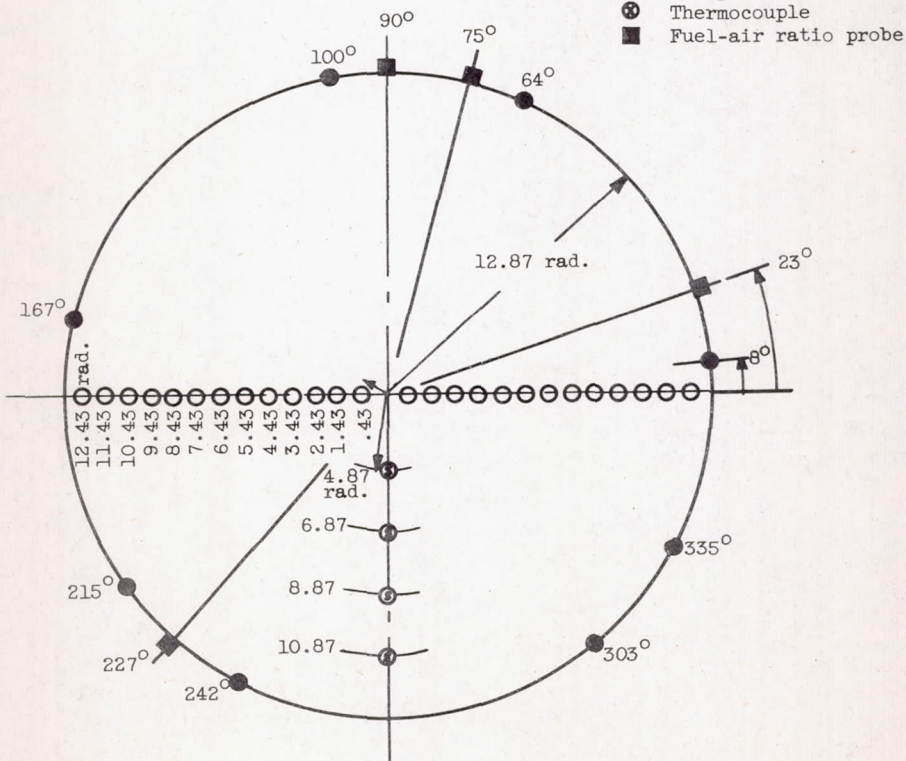


(c) Vortex generator spacing of flame holders 6, 8, and 9.

Figure 3. - Concluded. Flame-holder geometry. (Dimensions are in inches.)

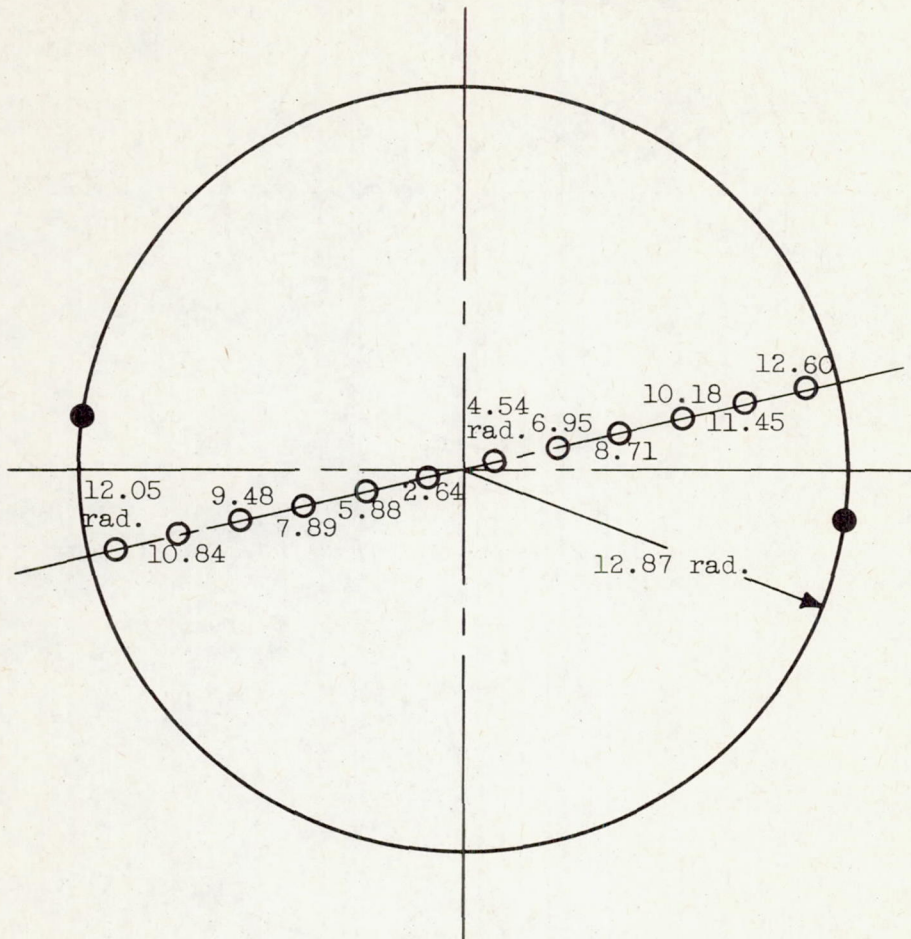


(a) Station 2.



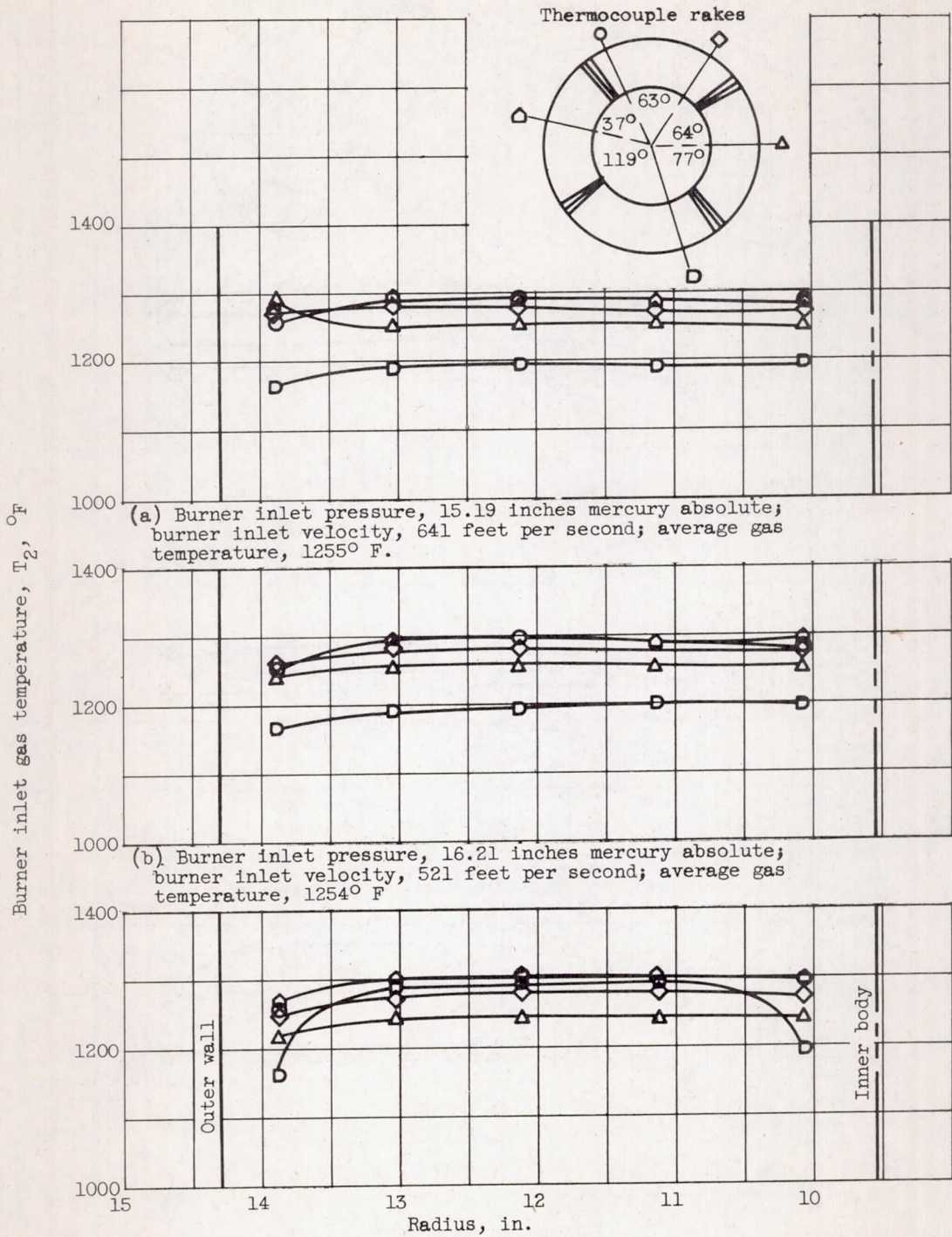
(b) Station 4.

Figure 4. - Schematic diagram of instrumentation stations. (View looking downstream.)



(c) Station 5.

Figure 4. - Concluded. Schematic diagram of instrumentation stations. (View looking downstream.)



(c) Burner inlet pressure, 16.40 inches mercury absolute;
burner inlet velocity, 376 feet per second; average gas
temperature, 1266° F.

Figure 5. - Gas temperature distribution at station 2.

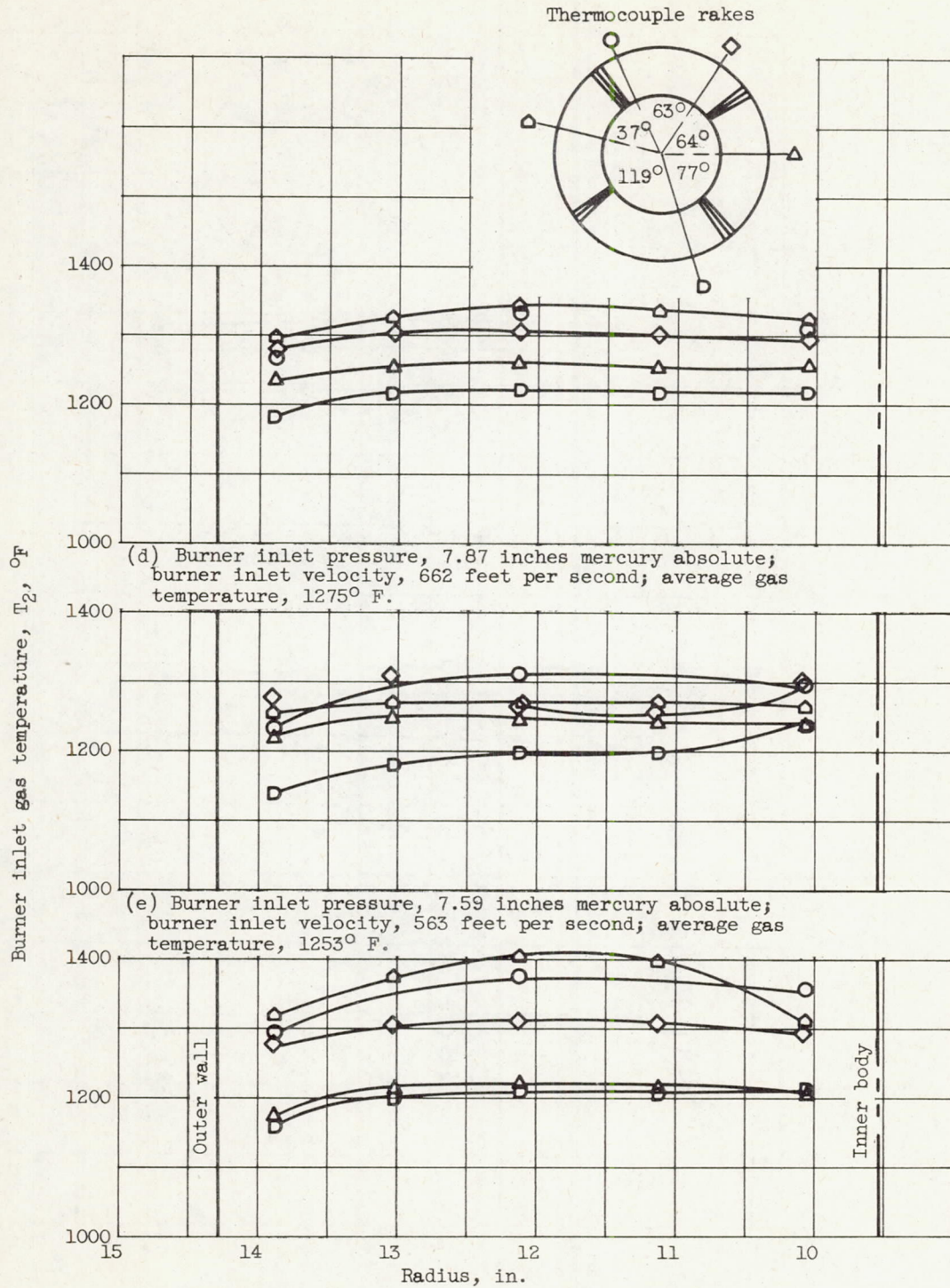


Figure 5. - Concluded. Gas temperature distribution at station 2.

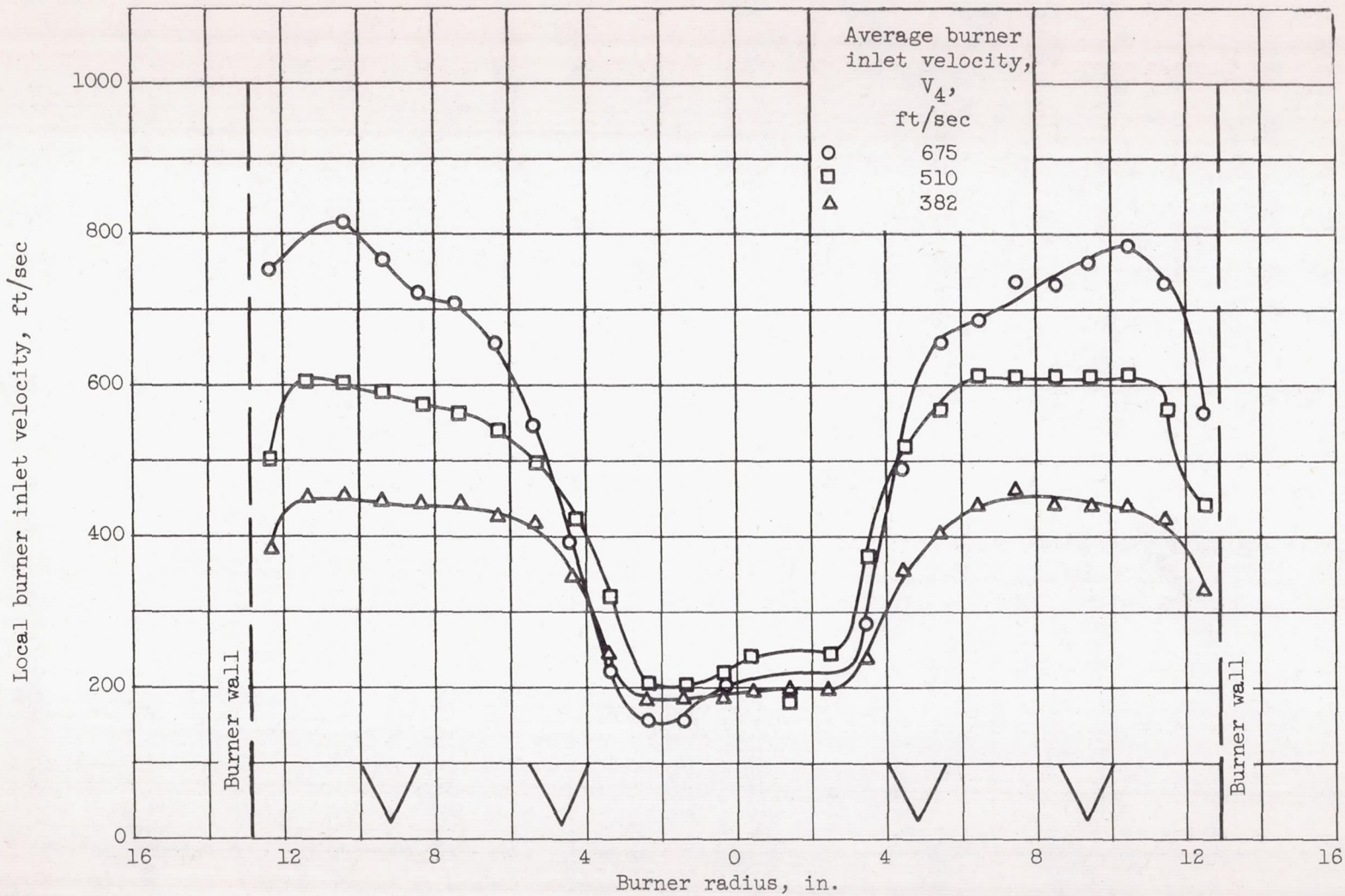
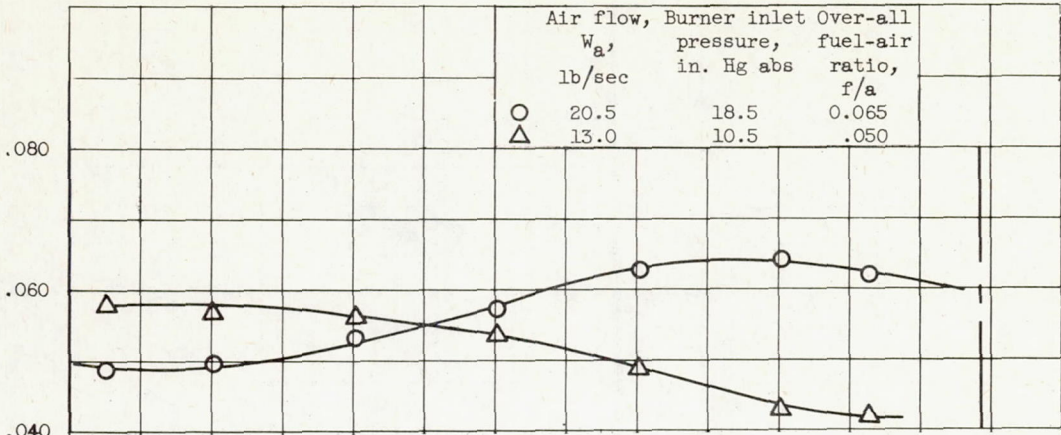
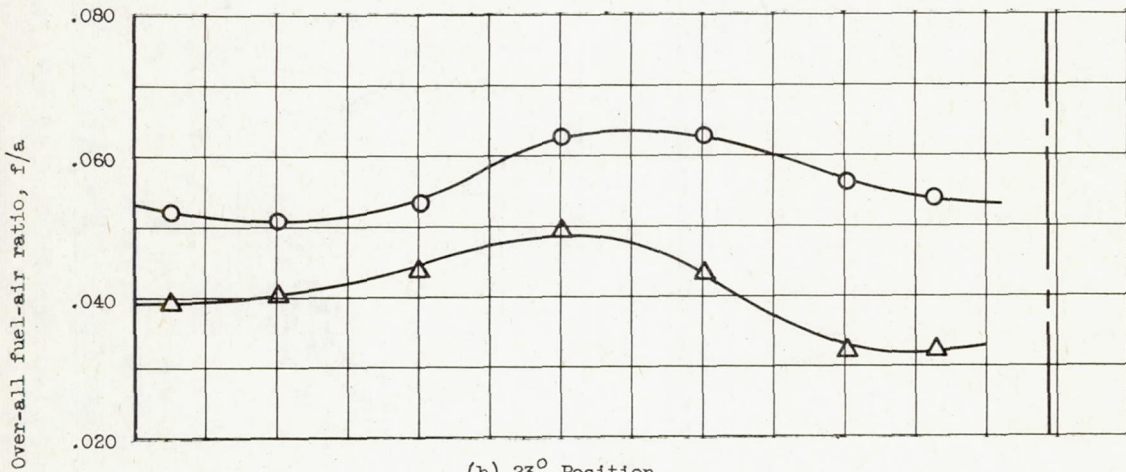


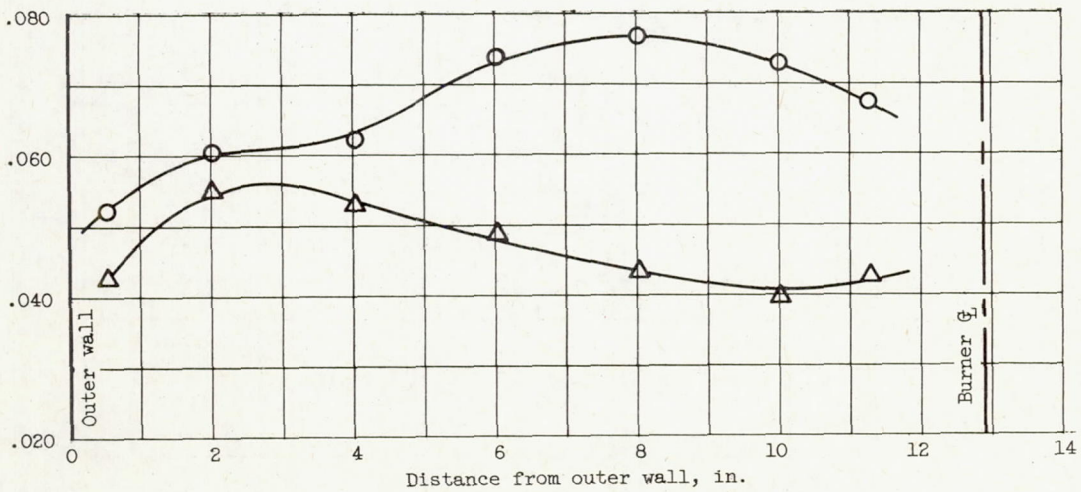
Figure 6. - Velocity profile at burner inlet (station 4) showing relative locations of flame-holder gutters. (View looking downstream.)



(a) 227° Position.



(b) 23° Position.



(c) 90° Position.

Figure 7. - Fuel-air distributions at burner inlet (station 4) at velocities of 480 to 520 feet per second.

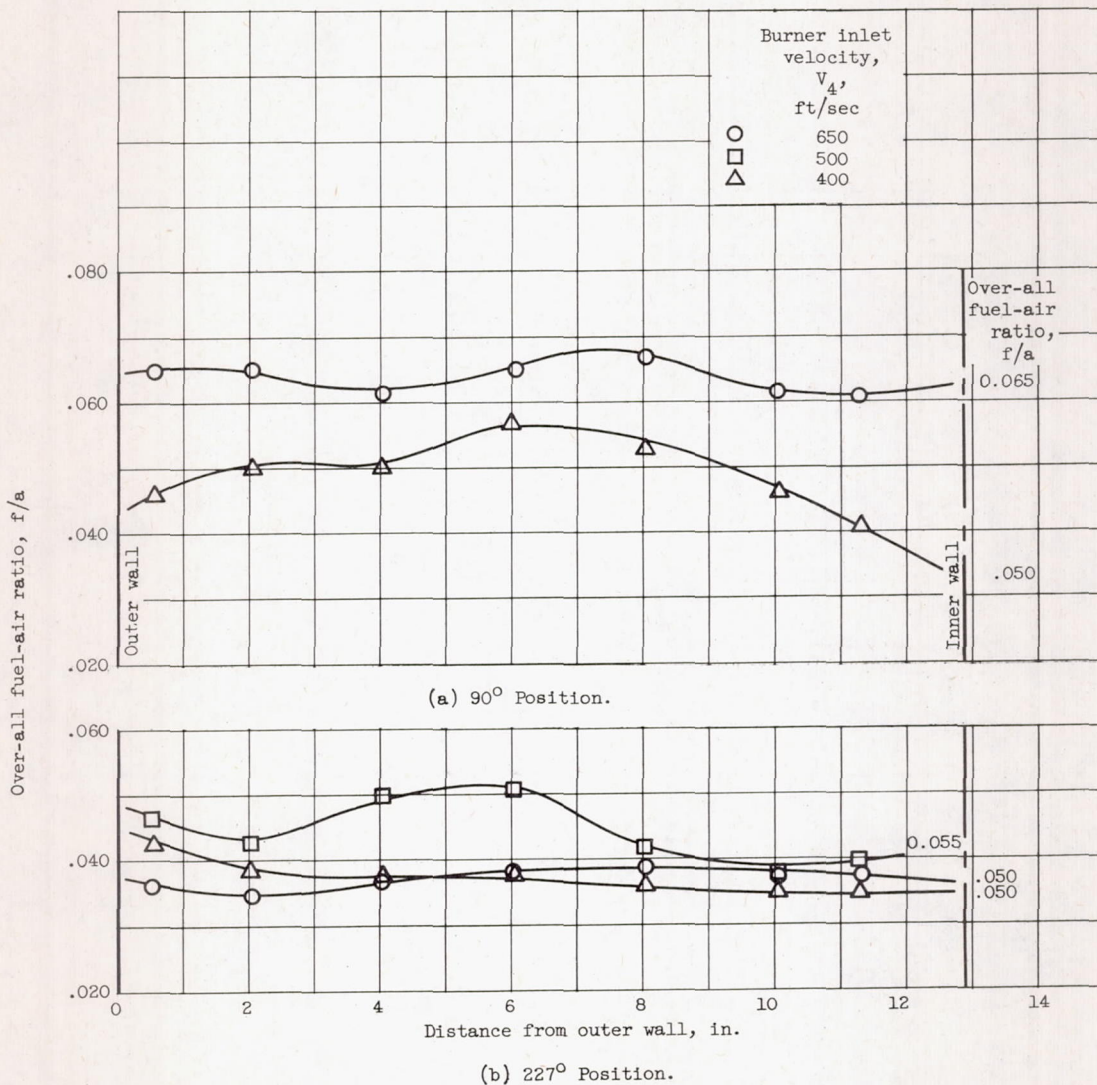
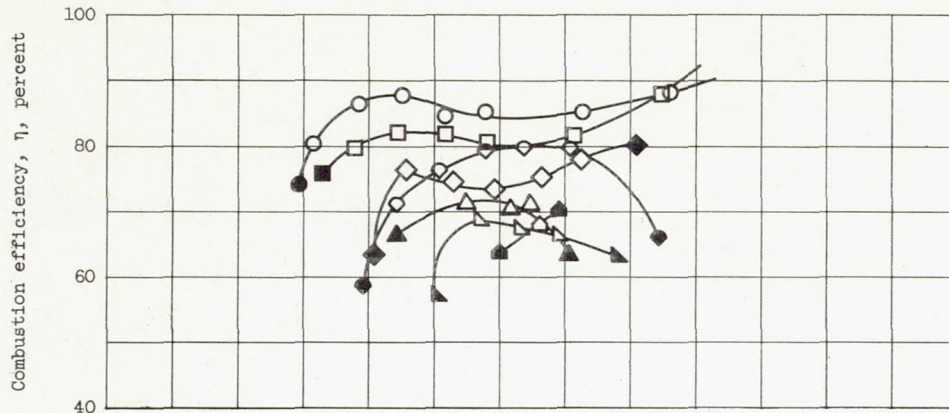
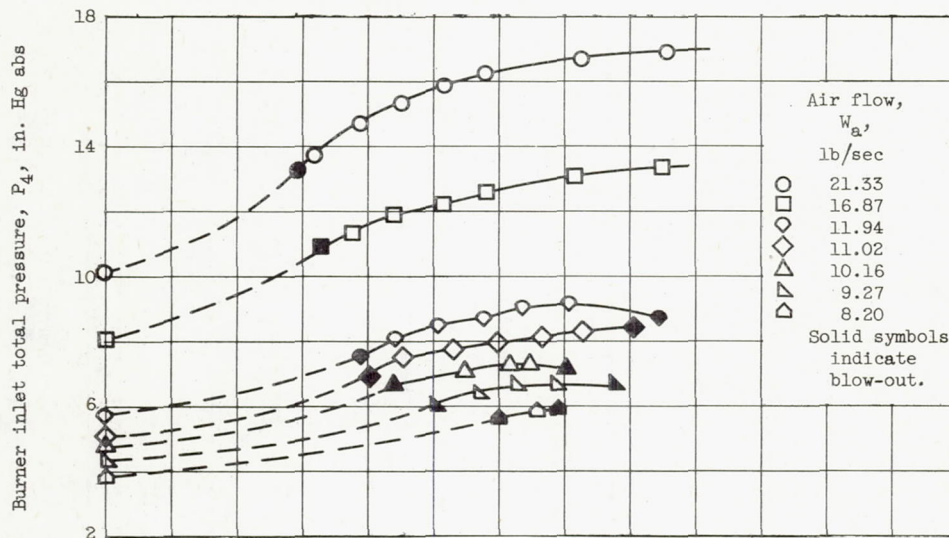


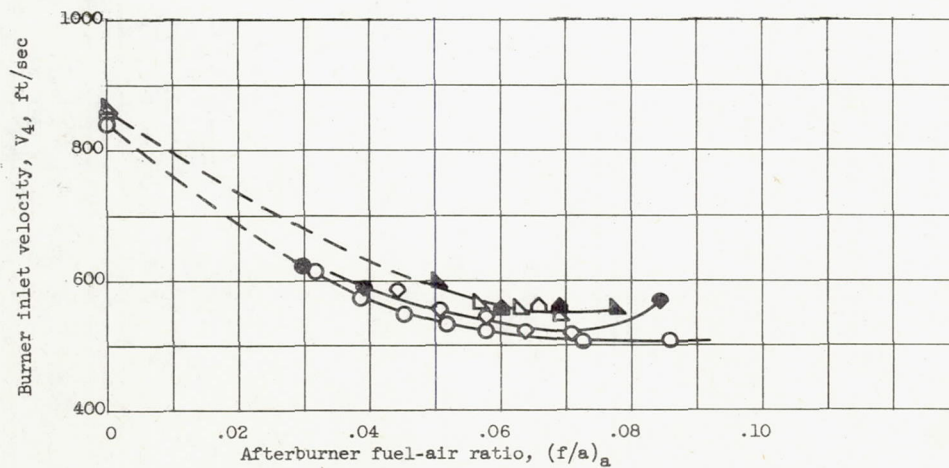
Figure 8. - Fuel-air distributions at burner inlet (station 4) for three velocity levels at air flow of 20 pounds per second.



(a) Combustion efficiency.

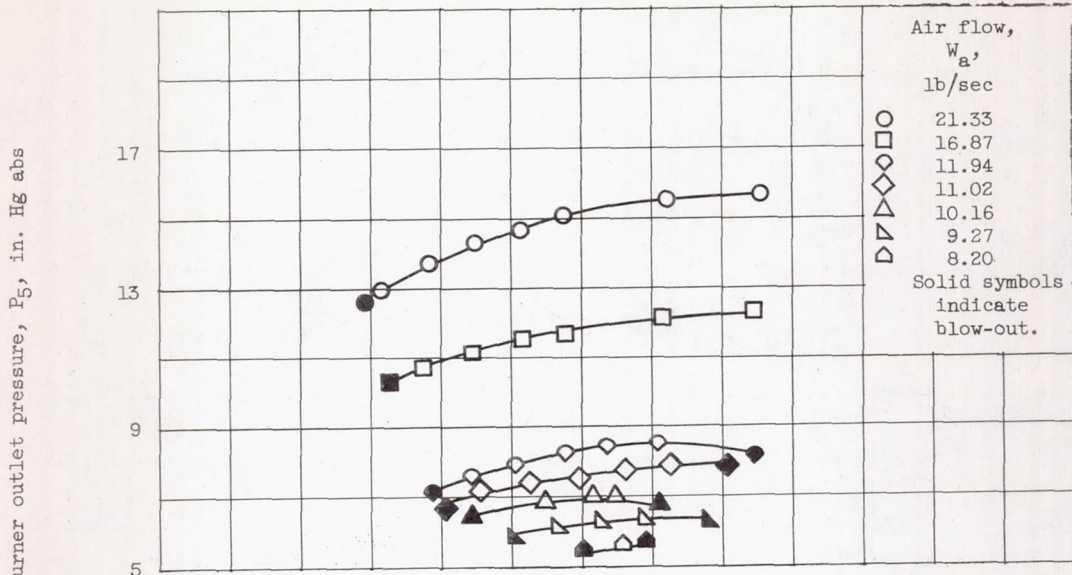


(b) Burner inlet pressure.

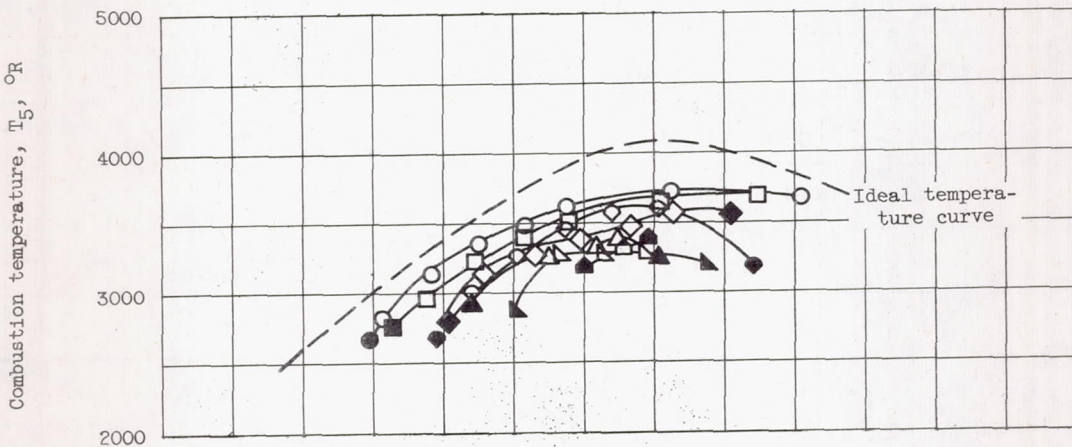


(c) Burner inlet velocity.

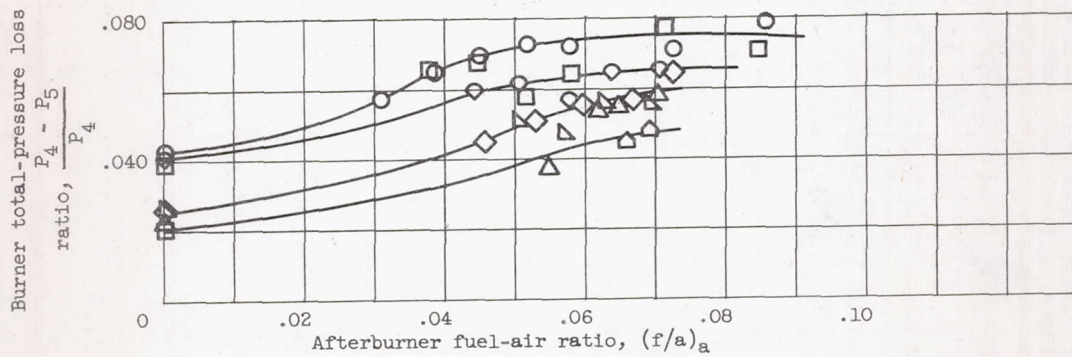
Figure 9. - Typical performance data with conventional V-gutters.



(d) Burner outlet pressure.



(e) Combustion temperature.



(f) Burner total-pressure loss ratio.

Figure 9. - Concluded. Typical performance data with conventional V-gutters.

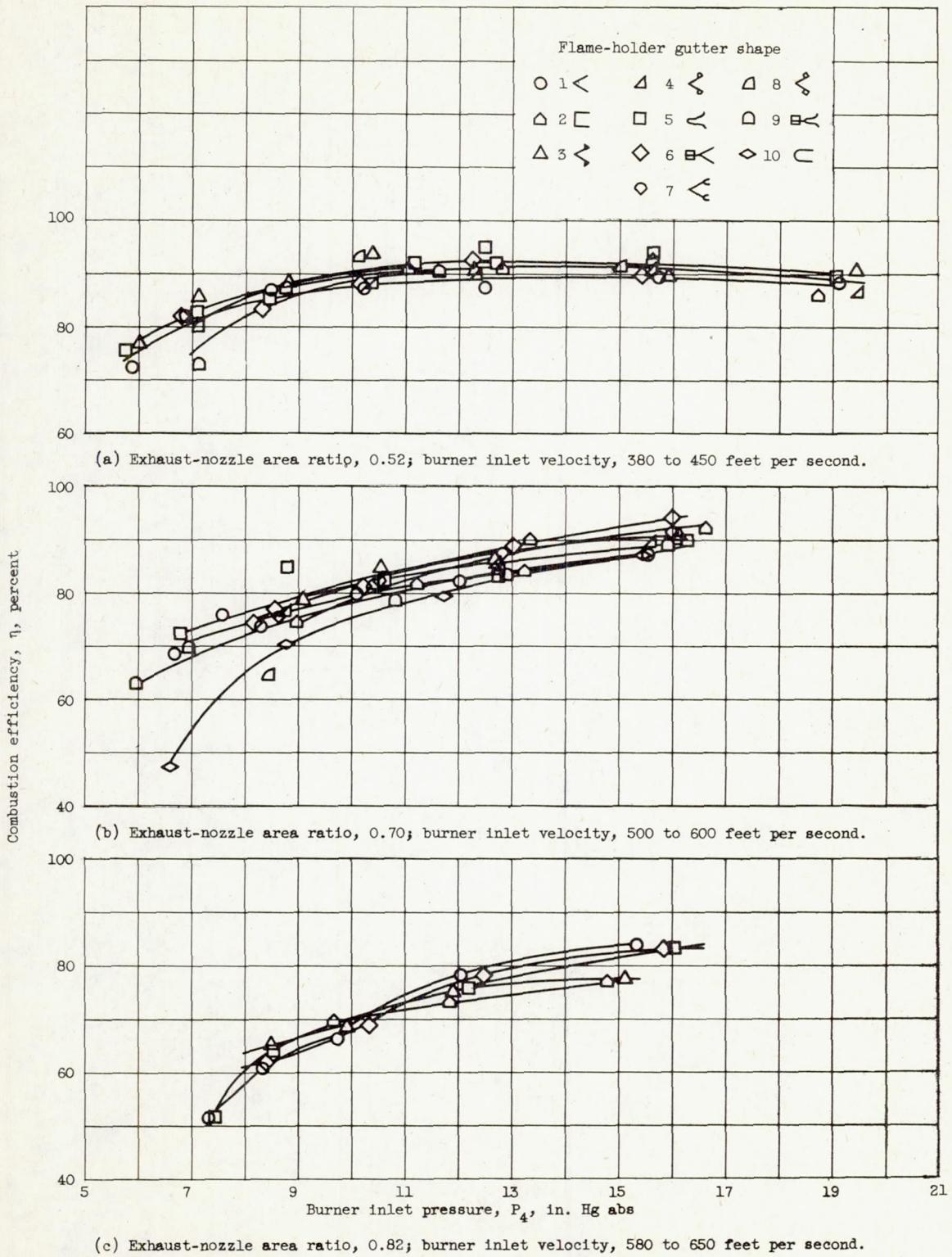
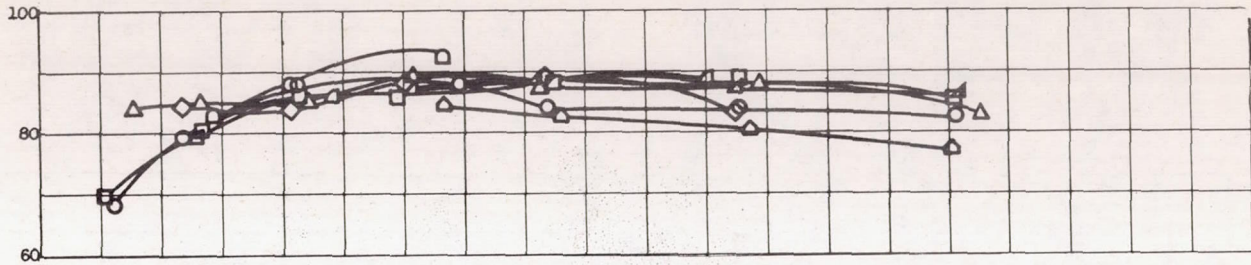
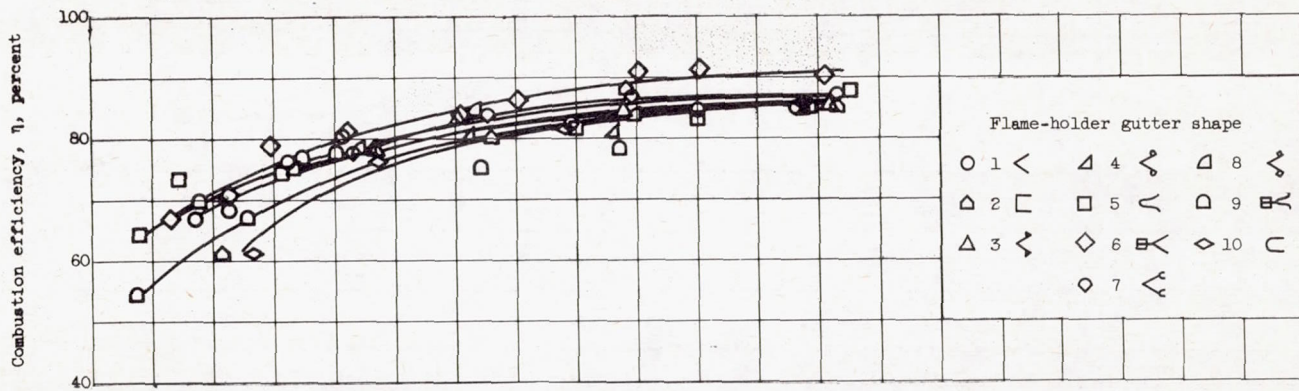


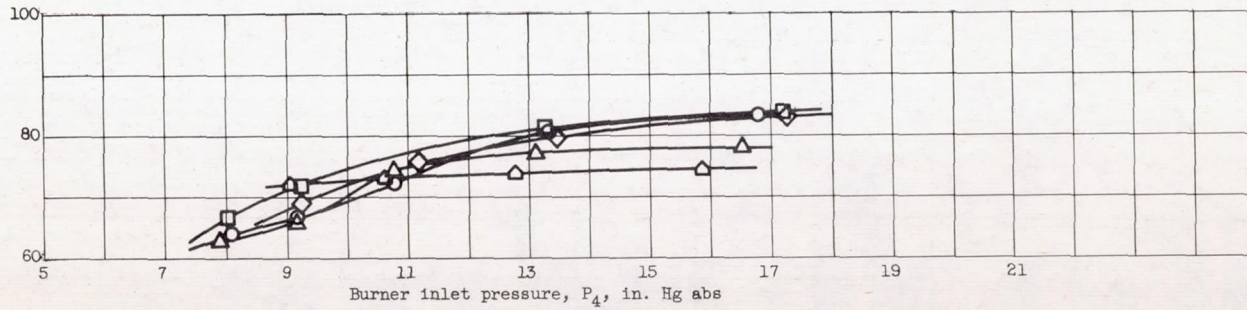
Figure 10. - Cross plot of combustion efficiency at fuel-air ratio of 0.047 for various burner inlet pressures.



(a) Exhaust-nozzle area ratio, 0.52; burner inlet velocity, 380 to 450 feet per second.



(b) Exhaust-nozzle area ratio, 0.70; burner inlet velocity, 500 to 600 feet per second.



(c) Exhaust-nozzle area ratio, 0.82; burner inlet velocity, 580 to 650 feet per second.

Figure 11. - Cross plot of combustion efficiency at fuel-air ratio of 0.067 for various burner inlet pressures.

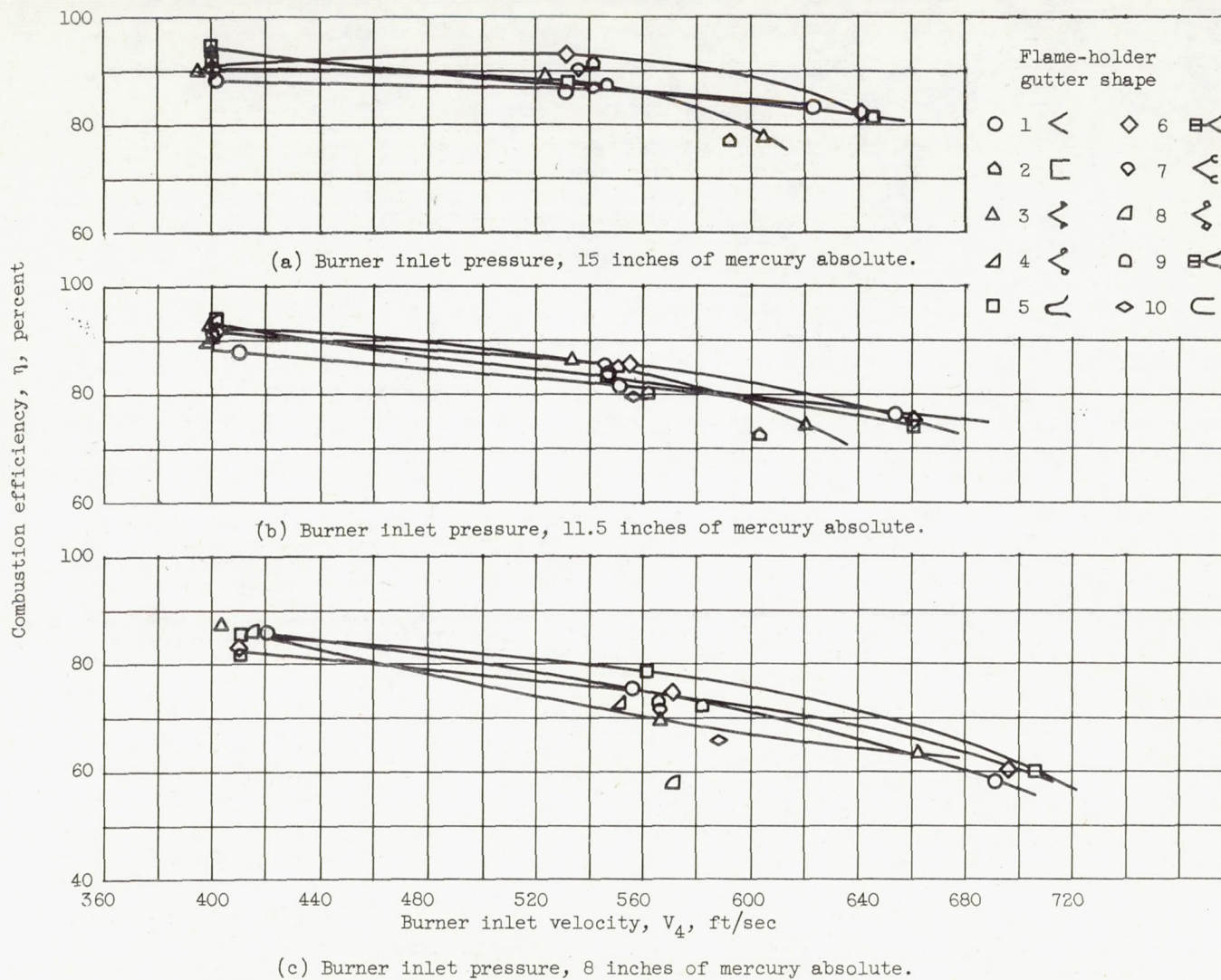


Figure 12. - The effect of burner inlet velocity on combustion efficiency at afterburner fuel-air ratio of 0.047 for various flame-holder shapes.

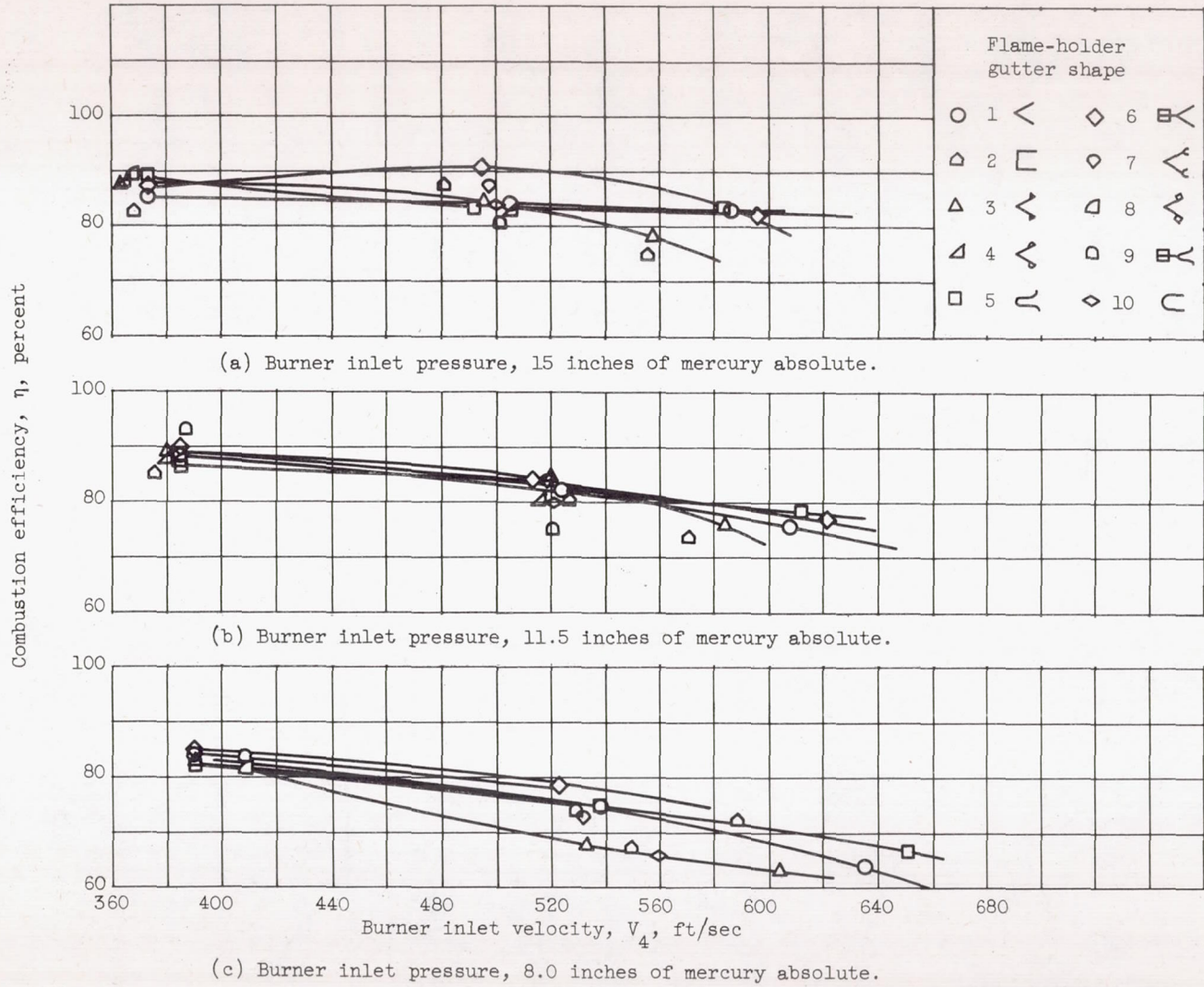


Figure 13. - The effect of burner inlet velocity on combustion efficiency at afterburner fuel-air ratio of 0.067 for various flame-holder shapes.

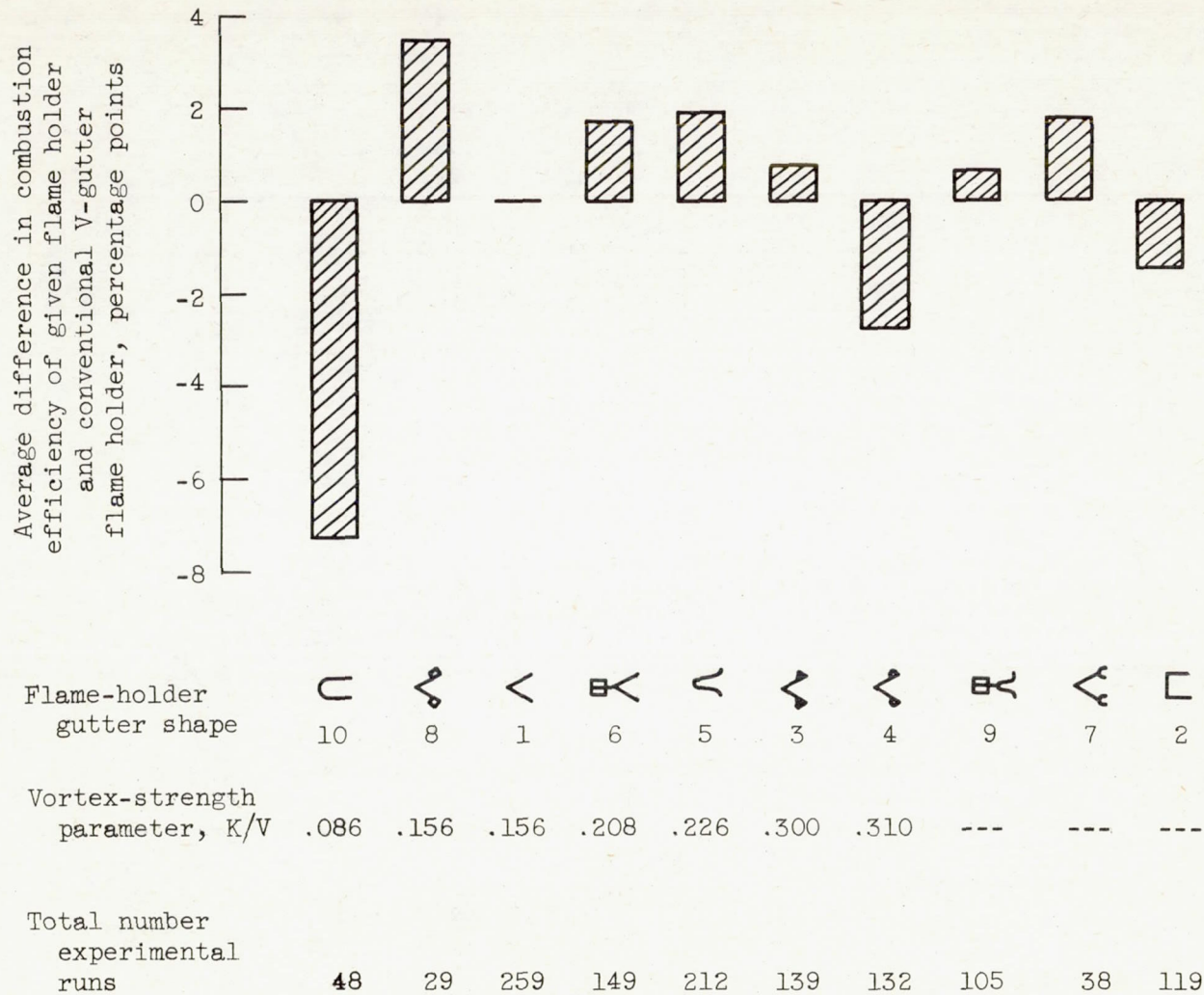


Figure 14. - Average differences between combustion efficiency of conventional V-gutter flame holder and combustion efficiencies of various flame-holder shapes.

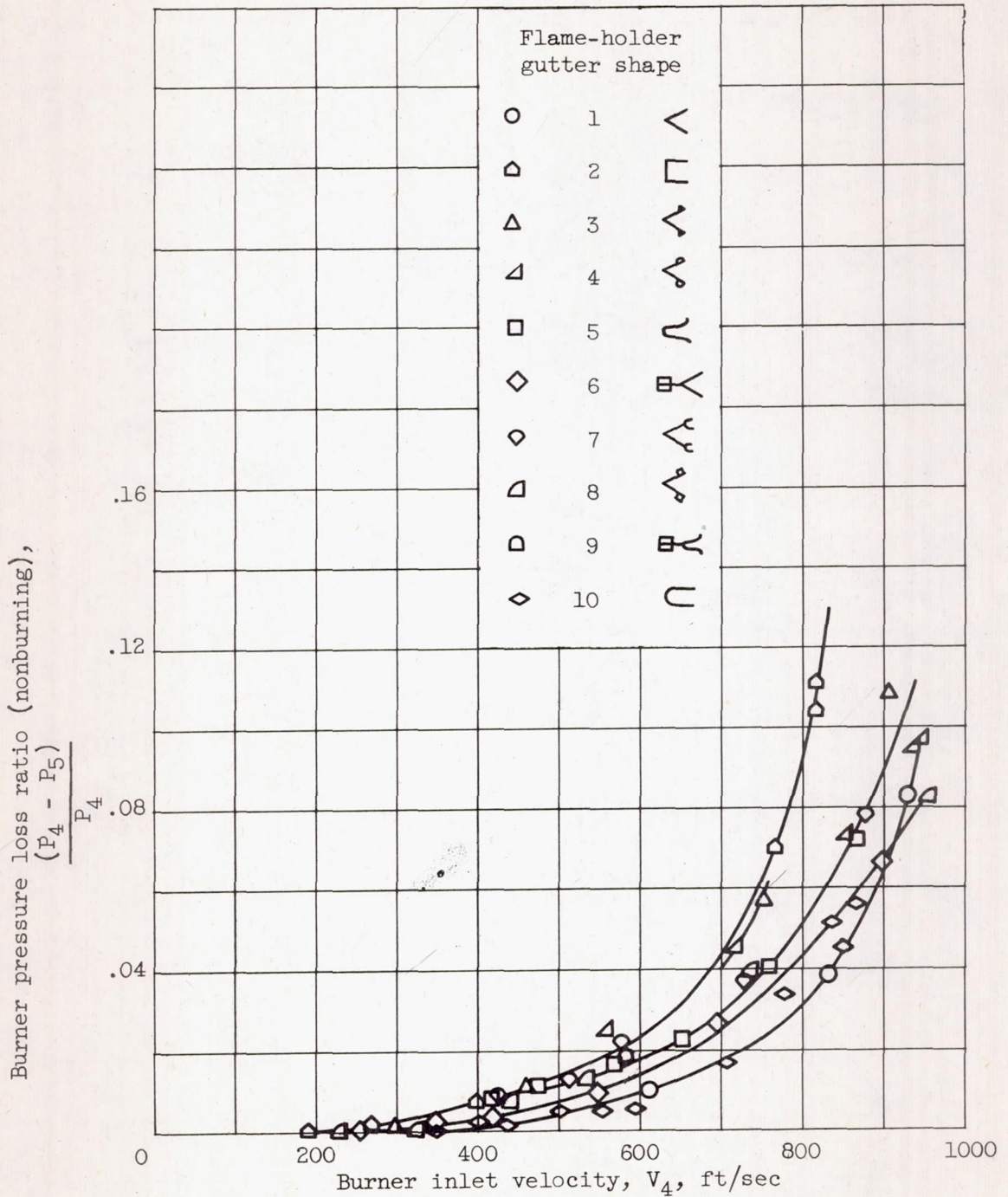
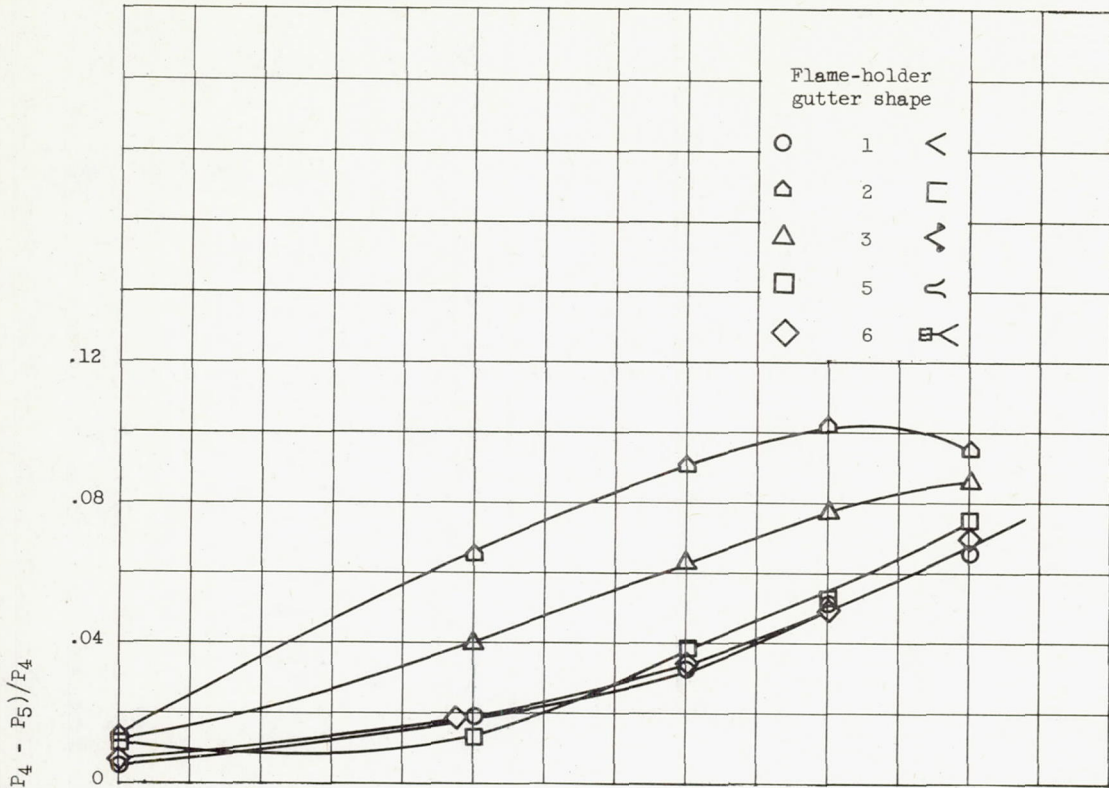
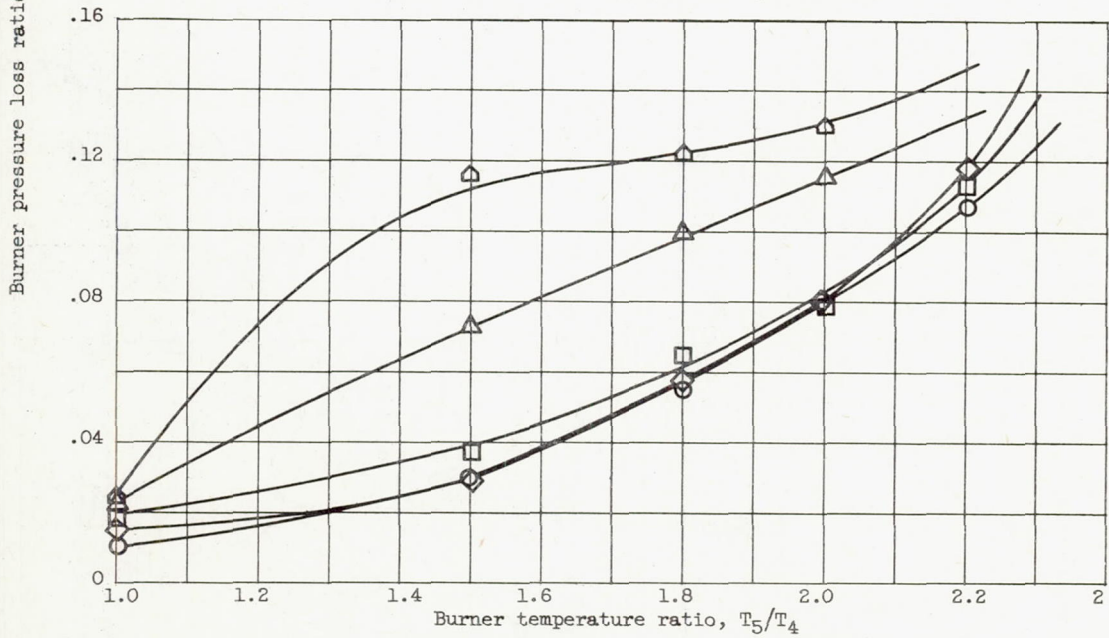


Figure 15. - Effect of burner inlet velocity on burner pressure loss ratio for various flame-holder gutter shapes without burning.



(a) Burner inlet velocity, 500 feet per second.



(b) Burner inlet velocity, 600 feet per second.

Figure 16. - Effect of burner temperature ratio and inlet velocity on burner pressure loss ratio for various gutter shapes with burning.

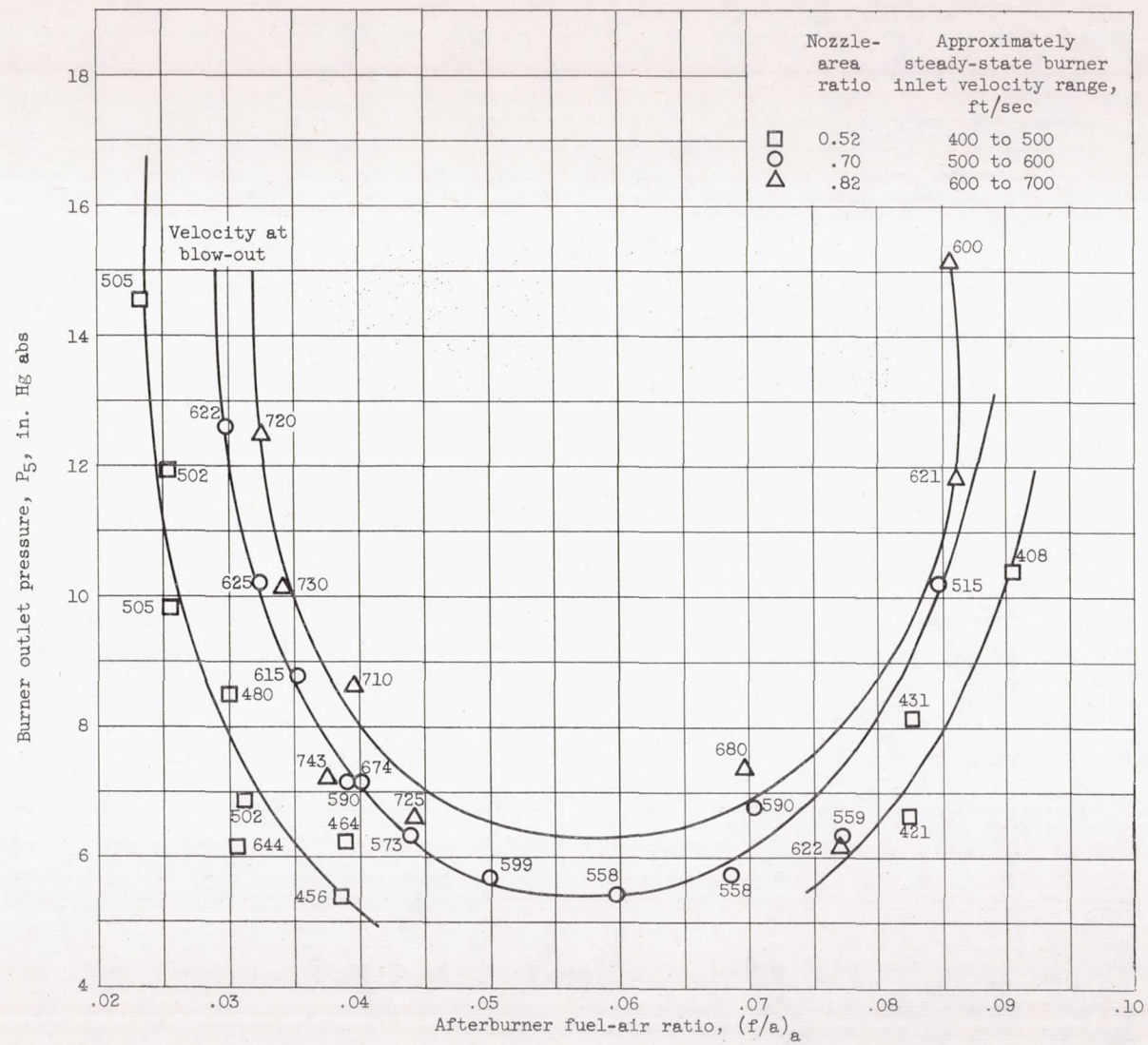


Figure 17. - Stability limits of flame-holder 1.

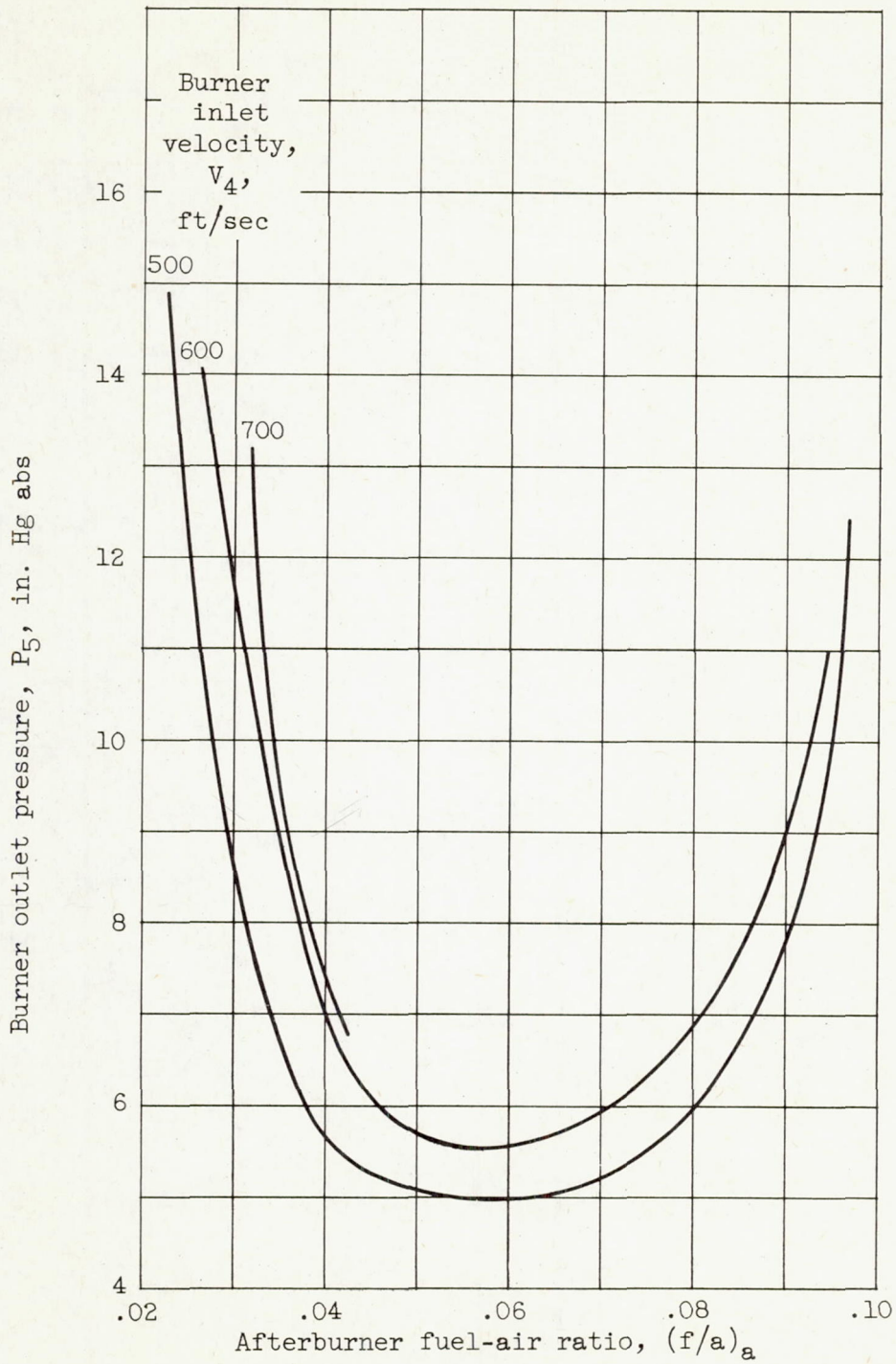


Figure 18. - Stability limits of flame holder 1 adjusted for velocity effect.

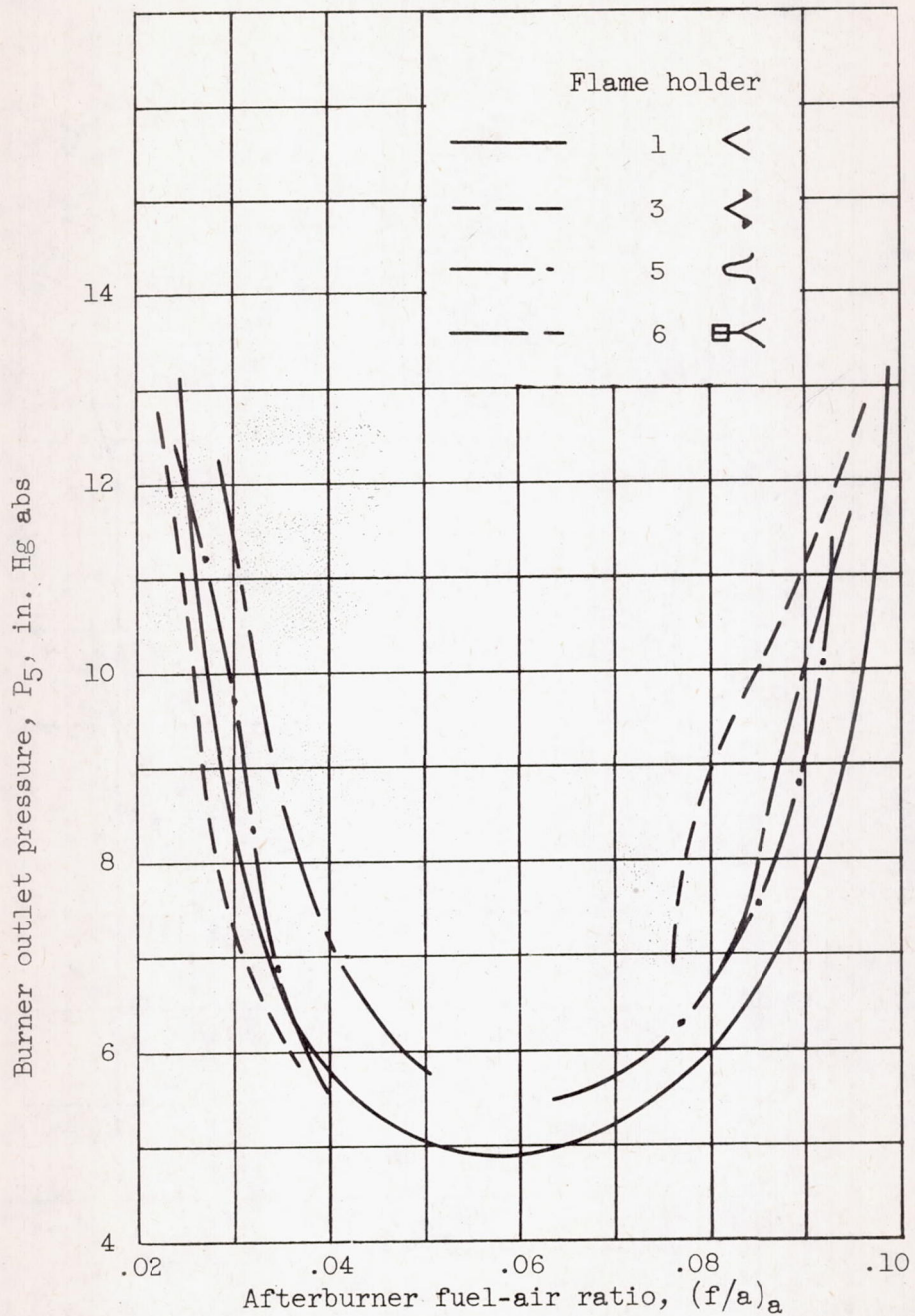


Figure 19. - Stability limits at burner inlet velocity of 500 feet per second for various flame-holder gutter shapes.

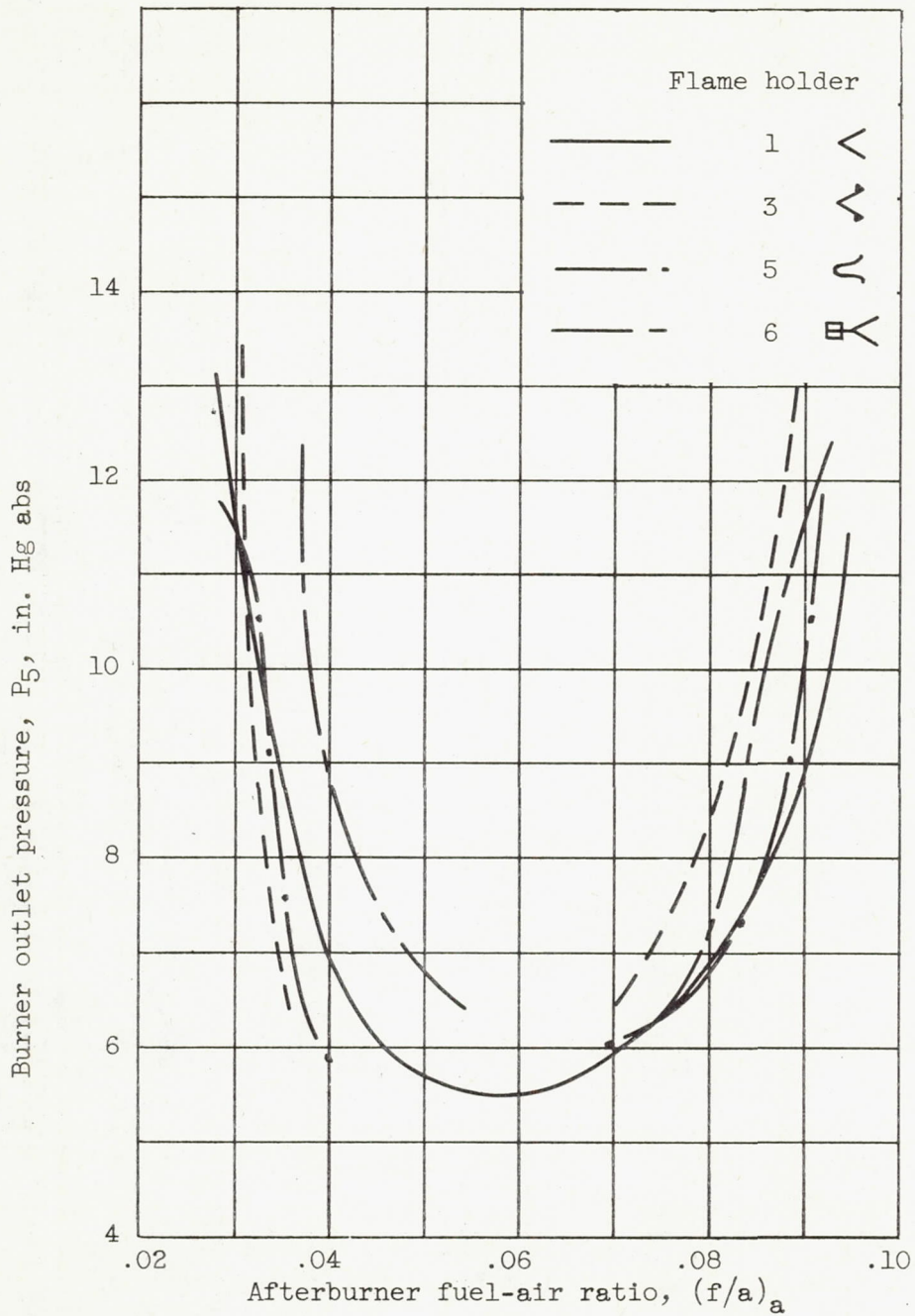


Figure 20. - Stability limits at burner inlet velocity of 600 feet per second for various flame-holder gutter shapes.

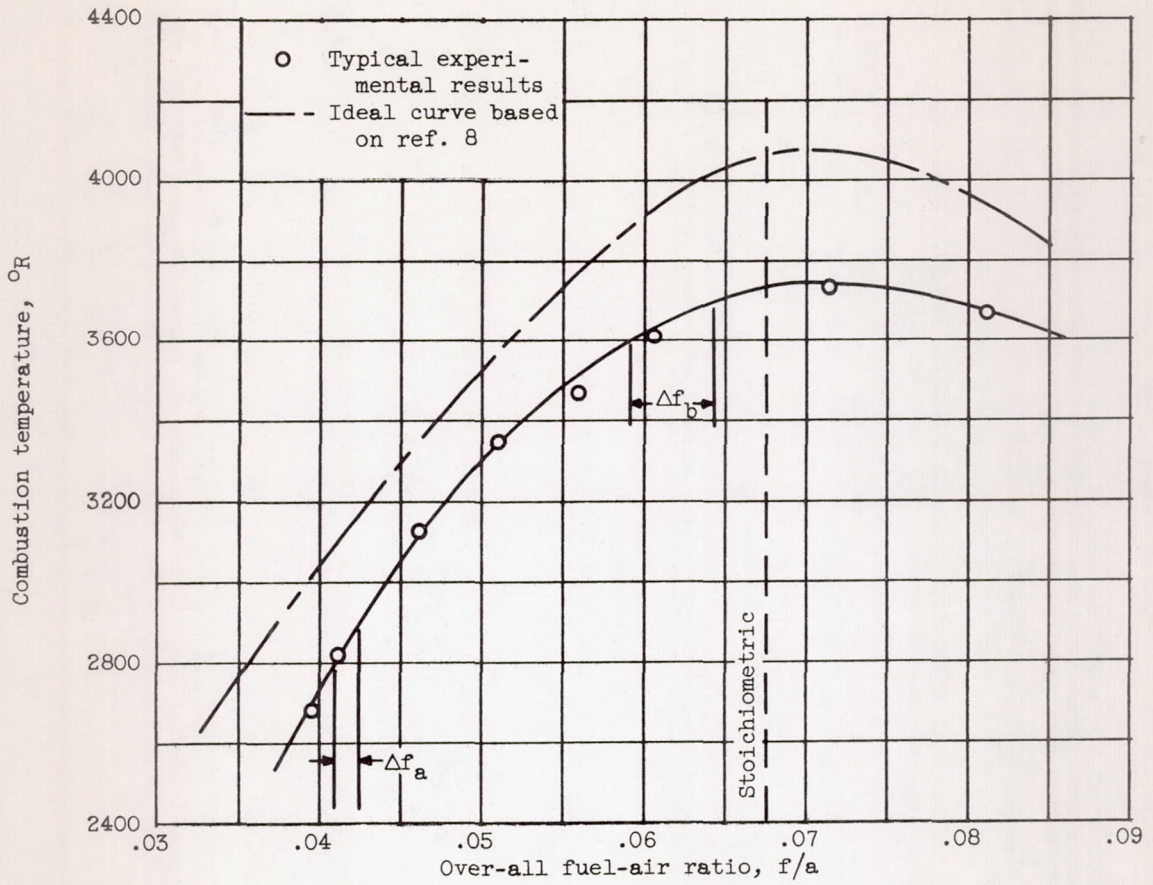


Figure 21. - Ideal and experimental combustion temperatures as function of over-all fuel-air ratio. Initial base temperature, 540° R.

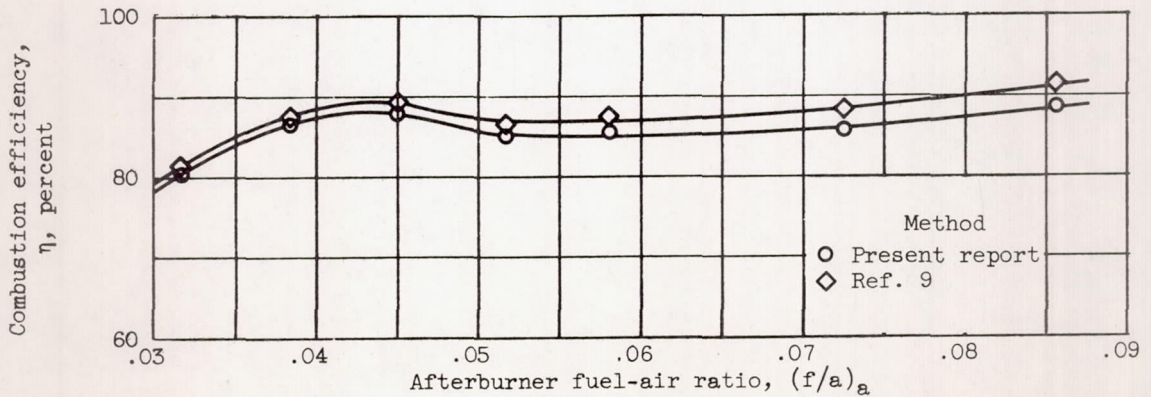
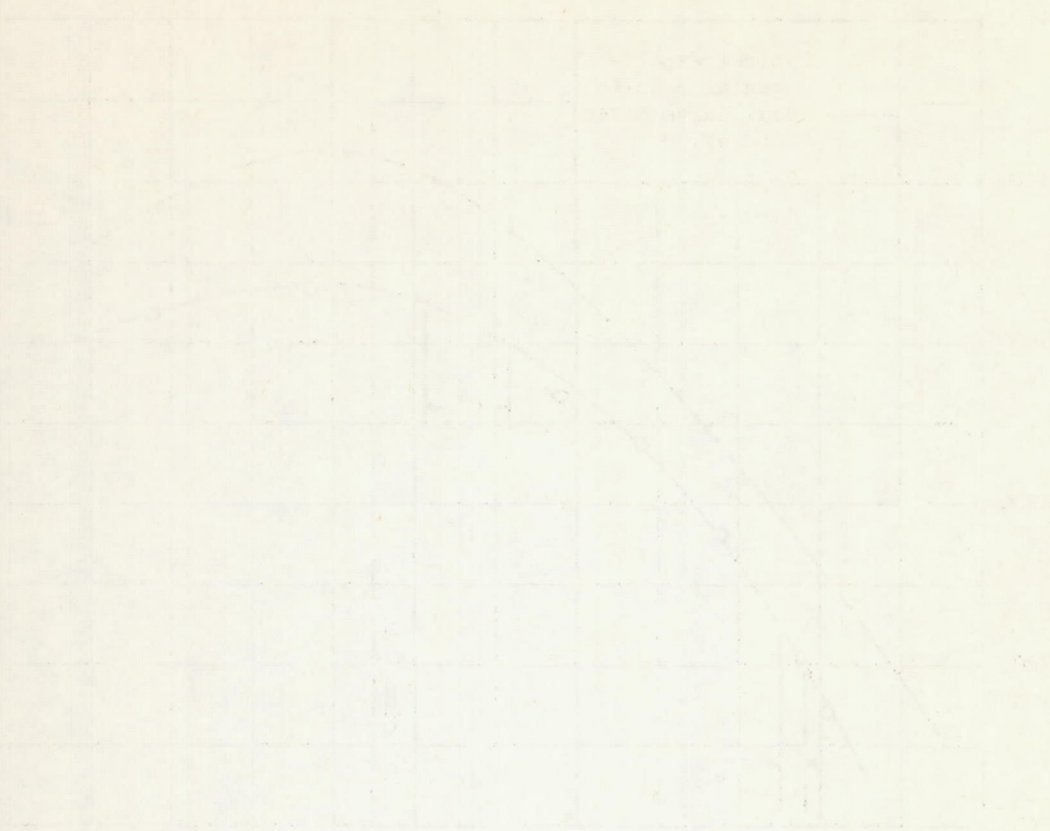


Figure 22. - Comparison of combustion efficiency calculated by two different methods as function of afterburner fuel-air ratio.



...